

PG-Flow: Deterministic implicit policy gradients for geometric product-form queueing networks *

Youssef Ait El Mahjoub¹

¹Efrei Research Lab, Université Paris-Panthéon-Assas, 30-32 Av. de la République, Villejuif, 94800, France.

Contributing authors: [youssef\[dot\]ait-el-mahjoub\[at\]efrei\[dot\]fr](mailto:youssef[dot]ait-el-mahjoub[at]efrei[dot]fr);

Abstract

Product-form queueing networks (PFQNs) admit steady-state distributions that factorize into local terms, and in many classical PFQNs—including Jackson, BCMP, G-networks, and Energy Packet Networks—these marginals are geometric and parametrized by local flow variables satisfying balance equations. While this structure yields closed-form expressions for key performance metrics, its use for deterministic steady-state optimization remains limited. We introduce *PG-Flow*, a deterministic policy-gradient framework that differentiates through the steady-state flow fixed-point equations, providing exact gradients via implicit differentiation and a local adjoint system while avoiding trajectory sampling and Poisson equations. We establish global convergence under structural assumptions (affine flow operators and convex local costs), and show that acyclic networks admit linear-time computation of both flows and gradients. Numerical experiments on routing control in Jackson networks and energy-arrival control in Energy Packet Networks demonstrate that PG-Flow provides a principled and computationally efficient approach to deterministic steady-state optimization in geometric product-form networks.

Keywords: Product-form queueing networks, Geometric steady-state distribution, Implicit policy gradient, Flow fixed points, Convex optimization

1 Introduction

Stochastic networks provide a fundamental framework for modeling the dynamics of complex systems such as communication infrastructures, manufacturing lines, and

*This manuscript is an extended preprint version of the under review document.

energy-aware sensor networks. Among these models, *product-form queueing networks* (PFQNs) occupy a central place due to their analytical tractability: under classical quasi-reversibility and independence conditions, their steady-state probability distribution factorizes into a product of local terms [1–3]. This property enables efficient computation of steady-state metrics such as throughput, occupancy, or delay, and has led to extensive work on performance evaluation and sensitivity analysis in both open and closed networks [4, 5]. More recently, the class of systems with product-form steady-state distributions has expanded through model-specific quasi-reversibility arguments, as in pass-and-swap queues [6]. Early contributions primarily focused on characterizing and evaluating steady-state behavior under fixed system parameters [1–4, 7–9].

As applications grew in scale and complexity, attention shifted from analysis to *control* and *optimization* of stochastic networks. In such settings, routing probabilities, service rates, or energy-allocation policies may be adjusted to improve long-run performance. This raises the challenge of optimizing steady-state metrics that depend implicitly on control parameters through the global balance equations of the network. In parallel, stochastic control and reinforcement learning have developed two major families of methods for optimizing decision-making in controlled Markov processes: value-based approaches and policy-based approaches [10, 11]. Value-based techniques, such as classical policy iteration, rely on repeated solutions of Poisson or Bellman equations to evaluate a fixed policy and then perform an improvement step. While theoretically sound, these methods become computationally intractable in large state spaces, motivating efforts to exploit structural decompositions of the underlying MDP. A first line of work addresses scalability through hierarchical MDPs, in which the decision problem is decomposed into subtasks; notable examples include MAXQ value-function decomposition [12] and hierarchical abstraction frameworks [13]. A complementary direction exploits factored or structured MDPs, where the transition and reward functions admit a graphical or algebraic decomposition, enabling low-dimensional value-function representations [14]. In the same spirit of leveraging structure for computational efficiency, several works have focused on structured decision processes arising in energy-aware systems, such as slot-based or superstate-decomposable MDPs [15–17], which allow scalable optimization in domains where standard DP becomes prohibitive. Despite these advances, these techniques rely on discrete state-action spaces and depend heavily on dynamic-programming operators. When the underlying dynamics or action spaces are continuous, these methods typically require approximation schemes, such as diffusion-based limits, linear approximation architectures, or neural-network parameterizations. To overcome such limitations, policy-based methods—most notably policy-gradient and actor–critic algorithms—estimate gradients directly from stochastic trajectories [18, 19]. More recently, implicit-differentiation techniques [20, 21] have enabled the computation of exact gradients through equilibrium constraints, bridging reinforcement learning with modern optimization theory.

Closer to product-form networks, several works have studied control based on interaction with the steady-state regime. Sanders et al. [22] proposed an online stochastic-approximation scheme for adjusting the parameters of a product-form

network using empirical steady-state observations. Their approach exploits the structural decomposition of PFQNs and relies on noisy gradient estimates obtained from time-window sampling. More recently, Comte and collaborators introduced the *Score-Aware Gradient Estimator (SAGE)* [23], a variance-reduced stochastic policy-gradient method based on Monte-Carlo sampling, applicable when the stationary distribution belongs to an exponential family (as in certain product-form systems). They establish local convergence in probability under the assumption that a suitable Lyapunov function exists. A complementary line of work focuses on controlling stochastic networks through Lyapunov-drift techniques, as developed by Neely [24]. This framework yields robust online algorithms—such as MaxWeight or drift-plus-penalty scheduling—that optimize long-run time averages without computing steady-state distributions. While highly effective for dynamic control, these approaches do not exploit product-form structures and do not address gradient-based steady-state optimization.

Despite these advances, existing methods lack *deterministic* gradient formulas that explicitly leverage the internal structure of product-form networks. In many classical PFQNs—including Jackson, BCMP, G-networks, and Energy Packet Networks—the steady-state distribution factorizes into geometric marginals parametrized by local flow variables. These flows satisfy a system of local balance equations linking arrival rates, service rates, activation probabilities, and routing. Although such equations are central to product-form derivations, they have been rarely used as the computational basis for policy optimization. Yet, in these models, performance metrics can be expressed solely in terms of local flow variables, enabling implicit differentiation through the associated equilibrium equations.

To address these limitations, we introduce *PG-Flow*, a framework for *deterministic policy-gradient optimization* tailored to product-form networks with geometric steady-state marginals. PG-Flow replaces global Poisson equations and sampling-based estimators with a system of local steady-state flow equations that implicitly characterize the long-run behavior of the network. Through implicit differentiation and the solution of a local adjoint system, PG-Flow computes exact gradients with quasi-linear complexity in the number of queues in certain structured cases. In the general setting, PG-Flow operates as a deterministic implicit-gradient method built upon the steady-state flow equations of a product-form network. Its computational and convergence properties are governed by the structural features of these flow equations: affine operators yield favorable convexity, while acyclic topologies induce triangular dependencies enabling efficient solvers. These structural regimes illustrate how analytical queueing-network models with product-form steady-state distributions can support scalable steady-state optimization. We conclude the introduction by summarizing our main contributions.

- We introduce a flow-based implicit-differentiation framework for geometric product-form networks: In PFQNs whose steady-state distribution factorizes into geometric marginals, several classical performance metrics such as queue length, delay, utilization, or leakage, admit natural closed-form expressions in terms of local steady-state flows. Building on this structure, we develop an

implicit-differentiation approach and present *PG-Flow*, a deterministic policy-gradient algorithm that computes exact steady-state gradients through the local equilibrium equations.

- We establish global convergence under structural assumptions and identify regimes of linear-time complexity: We prove that, under standard conditions (openness of the network, monotonicity of the flow operator, convexity of local costs, and in particular *affinity* of the steady-state flow equations), the steady-state performance objective becomes globally convex, and PG-Flow converges to the unique global minimizer. Furthermore, in *acyclic* networks the flow operator becomes triangular, making both the fixed-point computation and the adjoint solution reducible to back-substitution, and yielding an overall *linear-time* per iteration algorithm.
- We demonstrate PG-Flow on two representative control problems. We apply our framework to (i) a routing-control problem in an open Jackson network, and (ii) an energy-arrival control problem in an Energy Packet Network (EPN). These examples illustrate how PG-Flow exploits product-form structure to compute deterministic policy gradients efficiently in both classical and energy-aware queueing systems.

Table 1 summarizes the conceptual distinctions between existing approaches and the present work.

The remainder of the paper is organized as follows. Section 2 introduces the flow-based representation of geometric product-form networks and the associated steady-state fixed-point equations. Section 3 presents the PG-Flow algorithm, including the implicit-gradient formulation and the adjoint system. Section 4 establishes local and global convergence properties under structural assumptions, and Section 5 analyzes the computational complexity and identifies the acyclicity structure yielding linear-time implementations. Section 6 illustrates PG-Flow on routing control in an open Jackson network and on energy-arrival control in an Energy Packet Network. Section 7 concludes the paper and discusses perspectives for future research.

2 Steady-state flow problem

We consider an open stochastic network composed of d interacting queues and p control parameters. Each queue $i \in \{1, \dots, d\}$ is associated with a nonnegative *local steady-state flow variable* $\phi_i \in \mathbb{R}_+$, representing the steady-state intensity with which tasks (jobs, packets, or energy units, depending on the model) enter and leave that queue. Here, the term *steady-state flow* refers to the effective arrival/output rate of each queue in steady state. Under a control vector $\boldsymbol{\theta} \in \mathbb{R}^p$, this equilibrium flow is governed by a local operator $\mathcal{G}_i(\boldsymbol{\phi}; \boldsymbol{\theta})$, and collecting all components yields the global vector

$$\boldsymbol{\phi} = (\phi_1, \dots, \phi_d)^\top \in \mathbb{R}_+^d. \quad (1)$$

Table 1 Comparison of approaches for steady-state policy optimization in stochastic networks.

Method	Evaluation	Gradient	Use of product-form	Guarantees
Ref. [10]	Poisson / Bellman equation for policy evaluation	Not gradient-based; exact DP updates	None	Global optimality; monotone policy improvement
Ref. [24]	Lyapunov drift-plus-penalty based on queue backlog	No steady-state gradient; drift / subgradient-type control	None	Queue stability and asymptotic optimality of time averages
Ref. [22]	Empirical steady-state sampling over time windows	Stochastic gradient (Robbins-Monro)	Exploits product-form steady-state distribution (incl. normalization)	Asymptotic convergence under mixing assumptions
Ref. [25]	Analytical and QNA-based performance formulas	No analytic gradient; simulated annealing over routes	No explicit product-form (fork-join FIFO / infinite-server network)	Heuristic optimization; no formal gradient convergence result
Ref. [23]	Monte-Carlo sampling of steady-state Markov chain	Score-based policy gradient (likelihood ratio, SAGE)	Requires product-form / Exponential-family steady-state	Stochastic (local) convergence w.h.p. under local Lyapunov-stability assumptions
PG-Flow (this work)	Local steady-state flow equations with geometric marginals	Deterministic gradient (implicit differentiation + adjoint)	Explicitly uses product-form / Geometric-family steady-state	Local convergence in general; global under affine flows and (H1)–(H4); faster global convergence in acyclic networks

Product-form networks with geometric marginals.

In this work we focus on networks whose steady-state joint probability distribution admits a product-form representation with geometric marginals. Under a fixed policy $\boldsymbol{\theta}$, the steady-state probability of observing a state $x = (x_1, \dots, x_d)$ factorizes as

$$\Pi_{\boldsymbol{\theta}}(x) = \prod_{i=1}^d (1 - \rho_i^*(\boldsymbol{\theta})) \rho_i^*(\boldsymbol{\theta})^{x_i}, \quad (2)$$

where $\rho_i^*(\boldsymbol{\theta}) \in [0, 1]$ denotes the load of queue i in steady state. This geometric form arises in several well-established product-form models, including Jackson networks, BCMP queues, G-networks, and Energy Packet Networks (EPNs). In each case, the

parameter $\rho_i^*(\boldsymbol{\theta})$ is typically a deterministic function of the local steady-state flow $\phi_i^*(\boldsymbol{\theta})$ and model-specific parameters as service rate or energy parameters of node i . Because the geometric marginal depends essentially on these flows, many standard steady-state performance measures (mean queue length, mean delay, loss rate, or energy efficiency, etc.) can be expressed directly in terms of the steady-state flows.

Steady-state flows via fixed-point relations.

Although the network admits a product-form distribution, explicit computation of the normalizing constant C is not required for steady-state analysis. Instead, the network dynamics enforce a system of fixed-point equations characterizing the steady-state flows. For each node i , the equilibrium relation takes the form

$$\phi_i^* = \mathcal{G}_i(\boldsymbol{\phi}^*; \boldsymbol{\theta}), \quad i = 1, \dots, d. \quad (3)$$

The operator \mathcal{G}_i incorporates the model-specific mechanisms that govern the flow through queue i . A compact notation is obtained by defining the global operator

$$\mathcal{G}(\boldsymbol{\phi}; \boldsymbol{\theta}) := (\mathcal{G}_1(\boldsymbol{\phi}; \boldsymbol{\theta}), \dots, \mathcal{G}_d(\boldsymbol{\phi}; \boldsymbol{\theta}))^\top, \quad (4)$$

so that the equilibrium flows satisfy the vector fixed-point equation

$$\boldsymbol{\phi}^*(\boldsymbol{\theta}) = \mathcal{G}(\boldsymbol{\phi}^*(\boldsymbol{\theta}); \boldsymbol{\theta}). \quad (5)$$

Solving (5) yields the steady-state flow vector $\boldsymbol{\phi}^*(\boldsymbol{\theta})$, from which the performance measures relevant to the optimization problem can be evaluated. The fixed-point representation therefore plays a fundamental role in our framework, serving as the sole interface between the controlled parameters and the steady-state behavior of the network. For instance, in a Jackson network with $M/M/1$ queues, and a control on routing probabilities $P(\boldsymbol{\theta})$, the steady-state flow satisfies

$$\phi_i(\boldsymbol{\theta}) = \lambda_i^{\text{ext}} + \sum_{j=1}^d P_{j,i}(\boldsymbol{\theta}) \phi_j(\boldsymbol{\theta}), \quad (6)$$

and the mean queue length is $m_i(\phi_i^*) = \phi_i^* / (\mu_i - \phi_i^*)$. While in G-networks [3, 4, 7, 26] flows incorporate the effects of triggered customer, and further in Energy Packet Networks [8, 9, 27], ϕ_i^* incorporates both data flow and energy flow, which jointly determine the steady-state occupancy of each node.

Steady-state objective.

Because steady-state performance decomposes into local contributions, the global objective (i.e. reward) can be written as

$$J(\boldsymbol{\theta}) = \sum_{i=1}^d w_i r_i(\phi_i^*(\boldsymbol{\theta}), \boldsymbol{\theta}) = \mathcal{F}(\boldsymbol{\phi}^*(\boldsymbol{\theta}), \boldsymbol{\theta}), \quad (7)$$

where $\mathcal{F} : \mathbb{R}^d \times \mathbb{R}^p \rightarrow \mathbb{R}$ is continuously differentiable and $w_i \geq 0$ are importance weights. All dependence on steady-state performance therefore flows through the steady-state vector $\phi^*(\theta)$, which makes the fixed-point relation (5) the fundamental structural element for the proposed deterministic gradient-based optimization method.

Our aim is to determine a control vector θ^* that minimizes the steady-state objective (7). In a gradient-based approach, the direction $\nabla_{\theta} J(\theta)$ provides the information required to update θ and improve system performance [10, 11, 28]. However, the mapping $\theta \mapsto \phi^*(\theta)$ is defined *implicitly* through the nonlinear fixed-point system (5). Consequently, computing $\nabla_{\theta} J(\theta)$ requires handling the implicit dependence of ϕ^* on the control parameters, which cannot be written in closed form.

In the next section, we exploit this implicit structure to derive an *implicit policy-gradient formula*, which leads naturally to the proposed **PG-Flow** algorithm. For clarity, we also specify the dimension conventions that will be used throughout the derivations.

Table 2 Notation and dimensions used throughout the paper.

Symbol	Dimensions / Domain	Description
ϕ	$\mathbb{R}_+^{d \times 1}$	Vector of steady-state flow variables
$\phi^*(\theta)$	$\mathbb{R}_+^{d \times 1}$	Fixed point satisfying $\phi^* = \mathcal{G}(\phi^*; \theta)$
θ	$\mathbb{R}^{p \times 1}$	Policy parameter vector (controls)
$\mathcal{G}(\phi, \theta)$	$\mathbb{R}_+^{d \times 1}$	Global flow operator (mapping flows to flows)
$\partial_{\phi} \mathcal{G}$	$\mathbb{R}^{d \times d}$	Jacobian of \mathcal{G} w.r.t. flows
$\partial_{\theta} \mathcal{G}$	$\mathbb{R}^{d \times p}$	Jacobian of \mathcal{G} w.r.t. parameters
$\mathcal{F}(\phi, \theta)$	\mathbb{R}	Global performance objective
$\partial_{\phi} \mathcal{F}$	$\mathbb{R}^{1 \times d}$	Row gradient of \mathcal{F} w.r.t. flows
$\partial_{\theta} \mathcal{F}$	$\mathbb{R}^{1 \times p}$	Row gradient of \mathcal{F} w.r.t. parameters
$\frac{d\phi^*}{d\theta}$	$\mathbb{R}^{d \times p}$	Sensitivity of steady-state flows
y	$\mathbb{R}^{d \times 1}$	Adjoint variable solving $(I - \partial_{\phi} \mathcal{G})^{\top} y = (\partial_{\phi} \mathcal{F})^{\top}$
$\nabla_{\theta} J$	$\mathbb{R}^{1 \times p}$	Row gradient of objective

3 PG-Flow algorithm

Assumption 1 For the remainder of this work, we make the following assumptions, needed for the derivation of the implicit gradient:

- (i) For any admissible parameter vector θ , the flow solution $\phi^*(\theta)$ exists. This assumption will be shown to hold for open networks (see Section 4).
- (ii) The global operator $\mathcal{G}(\phi; \theta)$ is C^1 in both arguments. Its Jacobians $\partial_{\phi} \mathcal{G} \in \mathbb{R}^{d \times d}$ and $\partial_{\theta} \mathcal{G} \in \mathbb{R}^{d \times p}$ exist and are continuous.
- (iii) \mathcal{F} is continuously differentiable.

The previous section introduced the steady-state flow equations $\phi^*(\boldsymbol{\theta})$ and the corresponding performance objective $J(\boldsymbol{\theta})$. Optimizing this objective requires the gradient $\nabla_{\boldsymbol{\theta}} J(\boldsymbol{\theta})$. Because $\phi^*(\boldsymbol{\theta})$ depends implicitly on $\boldsymbol{\theta}$ through the fixed-point system, the derivative must be propagated through the equilibrium mapping \mathcal{G} . We now derive an exact expression for this gradient and show how it leads to an efficient algorithmic formulation.

Differentiating (7) using the chain rule yields

$$\nabla_{\boldsymbol{\theta}} J = \partial_{\boldsymbol{\theta}} \mathcal{F} + \partial_{\phi} \mathcal{F} \frac{d\phi^*}{d\boldsymbol{\theta}}, \quad (8)$$

where $\nabla_{\boldsymbol{\theta}} J \in \mathbb{R}^{1 \times p}$, $\partial_{\boldsymbol{\theta}} \mathcal{F} \in \mathbb{R}^{1 \times p}$, $\partial_{\phi} \mathcal{F} \in \mathbb{R}^{1 \times d}$, and $\frac{d\phi^*}{d\boldsymbol{\theta}} \in \mathbb{R}^{d \times p}$.

Proof By total differentiation of $J(\boldsymbol{\theta}) = \mathcal{F}(\phi^*(\boldsymbol{\theta}), \boldsymbol{\theta})$, we have

$$dJ = \partial_{\phi} \mathcal{F} d\phi^* + \partial_{\boldsymbol{\theta}} \mathcal{F} d\boldsymbol{\theta},$$

Since

$$d\phi^* = \left(\frac{d\phi^*}{d\boldsymbol{\theta}} \right) d\boldsymbol{\theta},$$

we obtain

$$dJ = \left[\partial_{\boldsymbol{\theta}} \mathcal{F} + \partial_{\phi} \mathcal{F} \frac{d\phi^*}{d\boldsymbol{\theta}} \right] d\boldsymbol{\theta}.$$

Identifying the coefficient of $d\boldsymbol{\theta}$ yields $\nabla_{\boldsymbol{\theta}} J = \frac{dJ}{d\boldsymbol{\theta}}$, which proves (8). \square

Closed-form differentiation vs. numerical recomputation.

By *closed-form* we mean an explicit expression for $\phi^*(\boldsymbol{\theta})$ that can be differentiated. In the considered networks, this is typically intractable. A naive alternative is to *recompute the fixed point* for perturbed parameters and approximate derivatives by **finite differences**

$$\frac{\partial J}{\partial \theta_j} \approx \frac{J(\boldsymbol{\theta} + \varepsilon \mathbf{e}_j) - J(\boldsymbol{\theta} - \varepsilon \mathbf{e}_j)}{2\varepsilon}, \quad j = 1, \dots, p. \quad (9)$$

which requires recomputing the steady-state flows $\phi^*(\boldsymbol{\theta} \pm \varepsilon \mathbf{e}_j)$ for *every* parameter direction. Since each evaluation of $J(\boldsymbol{\theta} \pm \varepsilon \mathbf{e}_j)$ requires a full solution of the fixed-point system (5), finite differences incur a cost proportional to $2p$ steady-state-flow solves per iteration, which rapidly dominates the computational complexity. Implicit differentiation avoids this computational increase: the fixed-point system is solved *once* per iteration to obtain $\phi^*(\boldsymbol{\theta})$, after which the local Jacobians $\partial_{\phi} \mathcal{G}$ and $\partial_{\boldsymbol{\theta}} \mathcal{G}$ are evaluated around that solution. Even when these Jacobians must be estimated numerically (e.g., by finite differencing the map \mathcal{G} itself), one only evaluates \mathcal{G} —not the full fixed-point equation—thus avoiding repeated global solves. This distinction is crucial: implicit differentiation separates the expensive operation (solve ϕ^* once) from cheaper local sensitivity computations, whereas finite differences repeatedly recompute the global equilibrium. Section 5 gives a full comparison of the resulting computational costs.

Implicit differentiation.

Instead of recomputing the fixed point for each perturbation of θ , we use the *implicit function theorem* ([11, Prop. A.25]). That is, differentiating (5) locally yields

$$\frac{d\phi^*}{d\theta} = (\mathbf{I} - \partial_\phi \mathcal{G})^{-1} \partial_\theta \mathcal{G}. \quad (10)$$

Substituting (10) into (8) yields the *implicit gradient*:

$$\nabla_\theta J = \partial_\theta \mathcal{F} + \partial_\phi \mathcal{F} (\mathbf{I} - \partial_\phi \mathcal{G})^{-1} \partial_\theta \mathcal{G}. \quad (11)$$

Adjoint.

Equation (11) involves the inverse of $\mathbf{I} - \partial_\phi \mathcal{G}$. Rather than forming this inverse explicitly which is numerically less stable, in practice we introduce an adjoint variable $\mathbf{y} \in \mathbb{R}^{d \times 1}$ defined as the solution of

$$(\mathbf{I} - \partial_\phi \mathcal{G})^\top \mathbf{y} = (\partial_\phi \mathcal{F})^\top. \quad (12)$$

This construction corresponds to applying the inverse $(\mathbf{I} - \partial_\phi \mathcal{G})^{-1}$ indirectly via the solution of the linear system (12). Hence, by right-multiplying (11) by the transpose of the associated linear system. The transpose appears because the gradients are *row* vectors while the adjoint system acts on *column* vector \mathbf{y} . Substituting the definition of \mathbf{y} into (11) gives the *compact implicit gradient*:

$$\nabla_\theta J = \partial_\theta \mathcal{F} + \mathbf{y}^\top \partial_\theta \mathcal{G}. \quad (13)$$

Thus, the adjoint \mathbf{y} evaluates $\partial_\phi \mathcal{F} (\mathbf{I} - \partial_\phi \mathcal{G})^{-1}$ without explicit inversion, by solving a single local linear system of size d .

The PG-Flow algorithm

By summarizing previous steps, we propose the following deterministic implicit policy-gradient algorithm:

Algorithm 1 PG-Flow: Policy Optimization via steady-state Flow Equations

Require: Initial parameters θ

- 1: **while** not converged **do**
- 2: Solve steady-state flows: $\phi^* = \mathcal{G}(\phi^*; \theta)$.
- 3: Evaluate the average cost: $J(\theta) = \sum_i w_i r_i(\phi^*; \theta)$.
- 4: Compute local derivatives: $\partial_\phi \mathcal{F}$, $\partial_\theta \mathcal{F}$, $\mathbf{G}_\phi = \partial_\phi \mathcal{G}$, $\mathbf{G}_\theta = \partial_\theta \mathcal{G}$.
- 5: Solve the adjoint: $(\mathbf{I} - \mathbf{G}_\phi)^\top \mathbf{y} = (\partial_\phi \mathcal{F})^\top$.
- 6: Global gradient: $\nabla_\theta J = \partial_\theta \mathcal{F} + \mathbf{y}^\top \mathbf{G}_\theta$.
- 7: Update: $\theta \leftarrow \theta - \eta \nabla_\theta J$.
- 8: **end while**

Sections 2–3 only require Assumption 1. In Section 4 we introduce additional structural conditions (H1–H4) under which the PG-Flow iteration converges globally to a steady-state optimum.

4 Global Convergence of PG-Flow

The PG-Flow algorithm is a gradient-based optimization scheme. As such, it may in general converge only to a *local* minimum of the steady-state objective $J(\boldsymbol{\theta})$. To guarantee convergence to a *global* optimum, it is therefore necessary to identify sufficient conditions under which $J(\boldsymbol{\theta})$ is *convex* on its control domain.

Let $\Phi := \mathbb{R}_+^d$ denote the nonnegative orthant, representing all admissible steady-state flow vectors, and let $\mathcal{U} \subset \mathbb{R}^p$ be a convex set of feasible control parameters (for instance a simplex when a global resource budget must be split across nodes, as in the EPN example). We focus on a broad class of stochastic networks—including Jackson, BCMP, G-networks, and energy-based product-form models—whose steady-state flows $\boldsymbol{\phi}^*(\boldsymbol{\theta}) \in \Phi$ satisfy an *affine* fixed-point relation:

$$\boldsymbol{\phi}^*(\boldsymbol{\theta}) = \mathcal{G}(\boldsymbol{\phi}^*(\boldsymbol{\theta}), \boldsymbol{\theta}), \quad \mathcal{G}(\boldsymbol{\phi}, \boldsymbol{\theta}) = A(\boldsymbol{\theta}) \boldsymbol{\phi} + b(\boldsymbol{\theta}), \quad (14)$$

Here:

- $\boldsymbol{\theta} \in \mathcal{U}$ denotes the tunable control parameters (routing probabilities, service rates, energy-injection rates, etc.).
- $A(\boldsymbol{\theta}) \in \mathbb{R}_+^{d \times d}$ encodes the internal propagation of steady-state flow. Its entry $A_{ij}(\boldsymbol{\theta})$ represents the contribution of the steady-state flow at node j to that of node i . In classical Jackson networks, $A(\boldsymbol{\theta})$ reduces exactly to the transpose routing matrix P^\top . In BCMP networks, its block structure represents class-transition probabilities. In G-networks, $A(\boldsymbol{\theta})$ may incorporate positive and negative triggered movements. In Energy Packet Networks (EPNs) (for instance [27]), $A(\boldsymbol{\theta})$ captures the steady-state DP flow propagation, which again reduces to P^\top for the Data Packet queue.
- $b(\boldsymbol{\theta}) \in \mathbb{R}_+^d$ collects all exogenous or self-generated contributions to the flow that are independent of the internal interactions represented by $A(\boldsymbol{\theta})$. In Jackson networks, $b(\boldsymbol{\theta})$ equals the external arrival rates. In BCMP or G-networks, it may include class-dependent arrivals or triggered events as signals. In EPNs, it includes the exogenous injections of data or energy packets.

Thus, the pair $(A(\boldsymbol{\theta}), b(\boldsymbol{\theta}))$ fully describes the internal flow propagation and the external inputs of the steady-state regime. This general affine representation encompasses a wide family of product-form networks and forms the basis for analyzing convexity and deriving global convergence guarantees for PG-Flow.

The global performance objective is expressed as a sum of local reward functions (7) where each r_i is related to queue $i \in \{1, \dots, d\}$. Our goal is to determine the optimal control vector

$$\boldsymbol{\theta}^* \in \arg \min_{\boldsymbol{\theta} \in \mathcal{U}} J(\boldsymbol{\theta}). \quad (15)$$

In the following, we introduce structural assumptions (H1)–(H4) under which $J(\boldsymbol{\theta})$ is convex on \mathcal{U} , ensuring that PG-Flow converges to the global minimizer $\boldsymbol{\theta}^*$.

- (H1) **Convex and compact:** The control set \mathcal{U} is compact and convex.
- (H2) **Openness:** For all $\boldsymbol{\theta} \in \mathcal{U}$, the network is open: from every queue there exists a directed path to a departure node, so that no closed communicating class of queues can retain flow indefinitely.
- (H3) **Monotonicity:** The mapping $\boldsymbol{\theta} \mapsto \phi^*(\boldsymbol{\theta})$ is continuous on \mathcal{U} and coordinate-wise non-decreasing.
- (H4) **Local rewards:** Each local reward $r_i(\phi_i, \boldsymbol{\theta})$ is convex in $(\phi_i, \boldsymbol{\theta})$ and non-decreasing in ϕ_i . For example, $r_i(\phi_i) = \phi_i/(\mu_i - \phi_i)$ on $[0, \mu_i]$.

Lemma 1 (Existence of steady-state flows) *If the network is open, then the steady-state flow vector ϕ^* exists and is unique.*

Proof Openness (H2) guarantees that no unit of flow can circulate indefinitely in the network. This property is ensured under either one of the following structural conditions on the nonnegative interaction matrix $A(\boldsymbol{\theta})$:

- (i) *Strictly sub-stochastic case:* there exists $\kappa < 1$ such that $\sum_{j=1}^d A_{i,j}(\boldsymbol{\theta}) \leq \kappa$ for all rows i . Then $\|A(\boldsymbol{\theta})\|_\infty \leq \kappa < 1$, so by Perron–Frobenius $\rho(A(\boldsymbol{\theta})) < 1$.
- (ii) *Feed-forward (acyclic) case:* $A(\boldsymbol{\theta})$ can be permuted into a strictly triangular form with zero diagonal (no self-loops and no cycles). Triangularity implies that all eigenvalues of $A(\boldsymbol{\theta})$ are zero, hence $\rho(A(\boldsymbol{\theta})) = 0$.

In both cases we obtain $\rho(A(\boldsymbol{\theta})) < 1$, which ensures that $\mathbf{I} - A(\boldsymbol{\theta})$ is invertible and that the Neumann series converges:

$$(\mathbf{I} - A(\boldsymbol{\theta}))^{-1} = \sum_{n=0}^{\infty} A(\boldsymbol{\theta})^n.$$

Therefore the fixed-point equation $\phi^*(\boldsymbol{\theta}) = A(\boldsymbol{\theta})\phi^*(\boldsymbol{\theta}) + b(\boldsymbol{\theta})$ admits the unique solution

$$\phi^*(\boldsymbol{\theta}) = (\mathbf{I} - A(\boldsymbol{\theta}))^{-1}b(\boldsymbol{\theta}) = \sum_{n=0}^{\infty} A(\boldsymbol{\theta})^n b(\boldsymbol{\theta}). \quad \square$$

Corollary 1 (Existence of adjoint solution) *The adjoint system (12) admits a unique solution.*

Proof From the affine form in (14), $\mathcal{G}(\phi; \boldsymbol{\theta}) = A(\boldsymbol{\theta})\phi + b(\boldsymbol{\theta})$, so that

$$\mathbf{G}_\phi(\boldsymbol{\theta}) = \frac{\partial \mathcal{G}(\phi; \boldsymbol{\theta})}{\partial \phi} = A(\boldsymbol{\theta}), \quad \forall \phi, \boldsymbol{\theta}.$$

and by Lemma 1, the matrix $I - A(\boldsymbol{\theta})$ is invertible for all $\boldsymbol{\theta}$, and therefore so is its transpose $(I - A(\boldsymbol{\theta}))^\top$. As a result, the adjoint system

$$(I - \mathbf{G}_\phi(\boldsymbol{\theta}))^\top \mathbf{y} = (I - A(\boldsymbol{\theta}))^\top \mathbf{y} = (\partial_\phi \mathcal{F}(\phi^*(\boldsymbol{\theta}), \boldsymbol{\theta}))^\top,$$

admits a unique solution $y(\boldsymbol{\theta}) \in \mathbb{R}^d$ for every $\boldsymbol{\theta} \in \mathcal{U}$. \square

Lemma 2 (Regularity and boundedness) *Let $\mathcal{U} \subset \mathbb{R}^p$ be compact. Assume that $A(\boldsymbol{\theta})$ is continuously differentiable in $\boldsymbol{\theta}$ on a neighborhood of \mathcal{U} . By Lemma 1, $I - A(\boldsymbol{\theta})$ is invertible for all $\boldsymbol{\theta} \in \mathcal{U}$. Then:*

- (a) *the mapping $\boldsymbol{\theta} \mapsto (I - A(\boldsymbol{\theta}))^{-1}$ is continuously differentiable on \mathcal{U} ;*
- (b) *the fundamental matrices are uniformly bounded:*

$$\sup_{\boldsymbol{\theta} \in \mathcal{U}} \|(I - A(\boldsymbol{\theta}))^{-1}\| < \infty.$$

Proof (a) Since $A(\boldsymbol{\theta})$ is C^1 , the map $\boldsymbol{\theta} \mapsto I - A(\boldsymbol{\theta})$ is C^1 . Lemma 1 ensures that $I - A(\boldsymbol{\theta})$ is invertible for every $\boldsymbol{\theta} \in \mathcal{U}$. For an invertible matrix M , the identity

$$\frac{d}{d\boldsymbol{\theta}}(M^{-1}(\boldsymbol{\theta})) = -M^{-1}(\boldsymbol{\theta}) M'(\boldsymbol{\theta}) M^{-1}(\boldsymbol{\theta})$$

holds whenever $M'(\boldsymbol{\theta})$ exists. Applying this with $M(\boldsymbol{\theta}) = I - A(\boldsymbol{\theta})$, we see that $(I - A(\boldsymbol{\theta}))^{-1}$ has a continuous derivative on \mathcal{U} , hence is C^1 .

(b) The map $\boldsymbol{\theta} \mapsto (I - A(\boldsymbol{\theta}))^{-1}$ is continuous on the compact set \mathcal{U} , so its norm attains a finite maximum. \square

Lemma 3 (Smoothness of the steady-state flow) *Let $\mathbf{b}(\boldsymbol{\theta})$ be continuously differentiable on a neighborhood of \mathcal{U} . For each $\boldsymbol{\theta} \in \mathcal{U}$, the steady-state flow is given by*

$$\phi^*(\boldsymbol{\theta}) = (I - A(\boldsymbol{\theta}))^{-1} \mathbf{b}(\boldsymbol{\theta}). \quad (16)$$

Under the assumptions of Lemma 2, the mapping $\boldsymbol{\theta} \mapsto \phi^(\boldsymbol{\theta})$ is C^1 on \mathcal{U} , and its Jacobian is uniformly bounded on \mathcal{U} :*

$$\sup_{\boldsymbol{\theta} \in \mathcal{U}} \|d\phi^*(\boldsymbol{\theta})\| < \infty. \quad (17)$$

Proof From Lemma 2, the inverse matrix $(I - A(\boldsymbol{\theta}))^{-1}$ is C^1 in $\boldsymbol{\theta}$ and its norm is uniformly bounded on \mathcal{U} . Since $\mathbf{b}(\boldsymbol{\theta})$ is also C^1 , the product $\phi^*(\boldsymbol{\theta}) = (I - A(\boldsymbol{\theta}))^{-1} \mathbf{b}(\boldsymbol{\theta})$ is C^1 as a composition and product of C^1 mappings.

Using the standard product rule for matrix–vector functions,

$$d\phi^*(\boldsymbol{\theta}) = d((I - A(\boldsymbol{\theta}))^{-1}) \mathbf{b}(\boldsymbol{\theta}) + (I - A(\boldsymbol{\theta}))^{-1} d\mathbf{b}(\boldsymbol{\theta}).$$

Each term on the right-hand side is continuous on the compact set \mathcal{U} :

- $(I - A(\boldsymbol{\theta}))^{-1}$ is continuous and uniformly bounded (Lemma 2),
- $d((I - A(\boldsymbol{\theta}))^{-1})$ is continuous on \mathcal{U} (Lemma 2(a)),
- $\mathbf{b}(\boldsymbol{\theta})$ and $d\mathbf{b}(\boldsymbol{\theta})$ are continuous by assumption.

A continuous function on a compact set is bounded. Hence both terms above are uniformly bounded on \mathcal{U} , and so is $d\phi^*(\boldsymbol{\theta})$. \square

Proposition 1 (Lipschitz continuity of the steady-state gradient) *Assume each local reward $r_i(\phi_i, \boldsymbol{\theta})$ is twice continuously differentiable on its domain. Define $J(\boldsymbol{\theta}) = \sum_{i=1}^d w_i r_i(\phi_i^*(\boldsymbol{\theta}), \boldsymbol{\theta})$, $w_i \geq 0$. Under Lemma 2 and Lemma 3, the mapping J is twice continuously differentiable on \mathcal{U} . Moreover, its Hessian is uniformly bounded on \mathcal{U} , i.e.*

$$L = \sup_{\boldsymbol{\theta} \in \mathcal{U}} \|\nabla^2 J(\boldsymbol{\theta})\| < \infty. \quad (18)$$

Consequently, the gradient ∇J is Lipschitz continuous on \mathcal{U} :

$$\|\nabla J(\boldsymbol{\theta}) - \nabla J(\boldsymbol{\theta}')\| \leq L \|\boldsymbol{\theta} - \boldsymbol{\theta}'\|, \quad \forall \boldsymbol{\theta}, \boldsymbol{\theta}' \in \mathcal{U}, \quad (19)$$

for some finite constant L .

Proof By Lemma 3, $\phi^*(\boldsymbol{\theta})$ is C^1 with uniformly bounded Jacobian on \mathcal{U} . Since each $r_i(\phi_i, \boldsymbol{\theta})$ is C^2 , the composite mapping $\boldsymbol{\theta} \mapsto r_i(\phi_i^*(\boldsymbol{\theta}), \boldsymbol{\theta})$ is also C^2 . Multiplying by a nonnegative constant w_i preserves C^2 -smoothness. Therefore the finite sum $J(\boldsymbol{\theta}) = \sum_{i=1}^d w_i r_i(\phi_i^*(\boldsymbol{\theta}), \boldsymbol{\theta})$ is C^2 on \mathcal{U} . Moreover, Each entry of $\nabla^2 J(\boldsymbol{\theta})$ is obtained from compositions and products of continuous functions (the partial derivatives of r_i , which are continuous by the C^2 assumption, and the derivative of ϕ^* , which is continuous by Lemma 3). Hence each entry of $\nabla^2 J(\boldsymbol{\theta})$ is continuous on the compact set \mathcal{U} and its norm achieves a finite maximum (18).

A standard result in smooth optimization then yields the Lipschitz continuity of the gradient: if the Hessian of a C^2 function is upper bounded by L on a convex set, then its gradient is L -Lipschitz on that set ([28, Eq. (9.13)]). Therefore,

$$J(\boldsymbol{\theta}') \leq J(\boldsymbol{\theta}) + \nabla J(\boldsymbol{\theta})^T (\boldsymbol{\theta}' - \boldsymbol{\theta}) + \frac{L}{2} \|\boldsymbol{\theta}' - \boldsymbol{\theta}\|^2,$$

and

$$\|\nabla J(\boldsymbol{\theta}) - \nabla J(\boldsymbol{\theta}')\| \leq L \|\boldsymbol{\theta} - \boldsymbol{\theta}'\|, \quad \forall \boldsymbol{\theta}, \boldsymbol{\theta}' \in \mathcal{U}.$$

Thus ∇J is L -Lipschitz on \mathcal{U} . \square

Theorem 1 (Convexity of J and global convergence of PG-Flow) *Under assumptions (H1)–(H4), the steady-state flow mapping $\boldsymbol{\theta} \mapsto \phi^*(\boldsymbol{\theta})$ defined by $\phi^* = A(\boldsymbol{\theta}) \phi^* + b(\boldsymbol{\theta})$ is well defined on \mathcal{U} . Moreover, with $w_i \geq 0$ the steady-state objective $J(\boldsymbol{\theta}) = \sum_{i=1}^d w_i r_i(\phi_i^*(\boldsymbol{\theta}), \boldsymbol{\theta})$ is convex on \mathcal{U} and admits at least one global minimizer $\boldsymbol{\theta}^* \in \arg \min_{\mathcal{U}} J$. In addition, J is continuously differentiable on \mathcal{U} and its gradient is Lipschitz continuous on \mathcal{U} . Therefore, for any initialization $\boldsymbol{\theta}_0 \in \mathcal{U}$, the PG-Flow iteration*

$$\boldsymbol{\theta}_{k+1} = \boldsymbol{\theta}_k - \eta_k \nabla J(\boldsymbol{\theta}_k) \quad (20)$$

with constant step-size $\eta_k \equiv \eta \in (0, 2/L)$, or with an Armijo backtracking rule, produces a non-increasing sequence $J(\boldsymbol{\theta}_k)$ and converges to a global minimizer of J on \mathcal{U} .

Proof Step 1 (Existence and uniqueness of steady-state flows). By Lemma 1 and Assumption (H2), $I - A(\boldsymbol{\theta})$ is invertible for all $\boldsymbol{\theta} \in \mathcal{U}$. Hence the fixed-point equation admits the unique solution $\phi^*(\boldsymbol{\theta}) = (I - A(\boldsymbol{\theta}))^{-1} b(\boldsymbol{\theta})$.

Step 2 (Existence of the adjoint solution). By Corollary 1, the adjoint system (12) admits a unique solution $y(\boldsymbol{\theta})$ for all $\boldsymbol{\theta} \in \mathcal{U}$, and the implicit gradient (13) $\nabla J(\boldsymbol{\theta})$ is therefore well defined.

Step 3 (Convexity of J). By Assumption (H3), $\boldsymbol{\theta} \mapsto \phi^*(\boldsymbol{\theta})$ is coordinatewise nondecreasing. By Assumption (H4), each local reward $r_i(x, \boldsymbol{\theta})$ is convex in $(x, \boldsymbol{\theta})$ and nondecreasing in x . Hence by composition with the monotone map ϕ_i^* , each function $\boldsymbol{\theta} \mapsto r_i(\phi_i^*(\boldsymbol{\theta}), \boldsymbol{\theta})$ is convex. Summing with $w_i \geq 0$ preserves convexity and yields the convexity of J on \mathcal{U} .

Step 4 (Differentiability and Lipschitz continuity of the gradient). By Lemma 3 the mapping $\boldsymbol{\theta} \mapsto \phi^*(\boldsymbol{\theta})$ is C^1 with uniformly bounded Jacobian on \mathcal{U} . Since each r_i is C^2 , Proposition 1 ensures that J is C^2 on \mathcal{U} , with a uniformly bounded Hessian (18). By the quadratic upper bound [28, Eq. (9.13)], ∇J is L -Lipschitz on \mathcal{U} .

Step 5 (Monotone descent and convergence). Since ∇J is L -Lipschitz, the "descent lemma" in [11, Prop. A.24] implies that for all x, y with $x, x + y \in \mathcal{U}$,

$$J(x + y) \leq J(x) + \nabla J(x)^T y + \frac{L}{2} \|y\|^2.$$

Applying (1) with $x = \boldsymbol{\theta}_k$ and $y = -\eta \nabla J(\boldsymbol{\theta}_k)$ yields

$$J(\boldsymbol{\theta}_{k+1}) = J(\boldsymbol{\theta}_k - \eta \nabla J(\boldsymbol{\theta}_k))$$

$$\begin{aligned}
&\leq J(\boldsymbol{\theta}_k) + \left(-\eta \nabla J(\boldsymbol{\theta}_k) \right)^\top \nabla J(\boldsymbol{\theta}_k) + \frac{L}{2} \left\| -\eta \nabla J(\boldsymbol{\theta}_k) \right\|^2 \\
&= J(\boldsymbol{\theta}_k) - \eta \left\| \nabla J(\boldsymbol{\theta}_k) \right\|^2 + \frac{L}{2} \eta^2 \left\| \nabla J(\boldsymbol{\theta}_k) \right\|^2 \\
&= J(\boldsymbol{\theta}_k) - \left(\eta - \frac{L}{2} \eta^2 \right) \left\| \nabla J(\boldsymbol{\theta}_k) \right\|^2.
\end{aligned} \tag{21}$$

Hence $\{J(\boldsymbol{\theta}_k)\}$ is non-increasing for any constant step-size $\eta \in (0, 2/L)$. Since J is convex on \mathcal{U} and has an L -Lipschitz continuous gradient, the standard convergence theory of gradient descent (see, e.g. [28, Sec. 9.1] or [11]) implies that $\boldsymbol{\theta}_k$ converges to a global minimizer $\boldsymbol{\theta}^* \in \arg \min_{\boldsymbol{\theta} \in \mathcal{U}} J(\boldsymbol{\theta})$. \square

Remark 1 (Projected PG-Flow under physical constraints) In many models the feasible control set $\mathcal{U} \subset \mathbb{R}^p$ is a compact convex subset reflecting physical limitations. Typical examples include:

- (i) constrained routing probabilities (section 6.1);
- (ii) admission or allocation rates constrained by capacity limits (section 6.2);
- (iii) energy allocation vectors subject to a global budget constraint (section 6.2), e.g.

$$\mathcal{U} = \left\{ \boldsymbol{\theta} \in \mathbb{R}_+^p : \sum_{i=1}^p \theta_i \leq B_{\max} \right\}. \tag{22}$$

The unconstrained PG-Flow update $\boldsymbol{\theta}_{k+1} = \boldsymbol{\theta}_k - \eta \nabla J(\boldsymbol{\theta}_k)$ may leave \mathcal{U} . To maintain feasibility, the update is replaced by the *Euclidean projected* iteration

$$\boldsymbol{\theta}_{k+1} = \Pi_{\mathcal{U}}(\boldsymbol{\theta}_k - \eta \nabla J(\boldsymbol{\theta}_k)), \quad \Pi_{\mathcal{U}}(x) = \arg \min_{u \in \mathcal{U}} \|u - x\|_2. \tag{23}$$

Convexity of \mathcal{U} ensures that $\Pi_{\mathcal{U}}$ is single-valued and non-expansive ($\|\Pi_{\mathcal{U}}(x) - \Pi_{\mathcal{U}}(y)\| \leq \|x - y\|$). Thus the descent arguments in the proof of Theorem 1 remain valid for the projected scheme, and global convergence continues to hold.

5 Computational Complexity Analysis

The computation of the steady-state objective $J(\boldsymbol{\theta})$ and its gradient depends critically on the method used to evaluate $\nabla_{\boldsymbol{\theta}} J$. Because J depends on the steady-state flow vector $\boldsymbol{\phi}^*(\boldsymbol{\theta})$, any gradient method must address two fundamental operations: (i) solving the steady-state fixed-point equation $\boldsymbol{\phi}^* = \mathcal{G}(\boldsymbol{\phi}^*; \boldsymbol{\theta})$ and (ii) propagating derivatives through the implicit dependence of $\boldsymbol{\phi}^*$ on $\boldsymbol{\theta}$. Different approaches treat these two operations very differently, which leads to significant variations in computational cost. In this section, we compare five gradient-estimation methods relevant to steady-state optimization in product-form queueing networks: finite differences applied to the full objective (FD-J), Monte-Carlo policy gradients, PG-Flow with numerical Jacobians, PG-Flow with analytical Jacobians, and finally PG-Flow in feed-forward networks. Each method reflects a distinct philosophy regarding how the steady state interacts with the control parameters, and therefore provides a different trade-off between accuracy, and computational efficiency.

Evaluating the steady-state objective $J(\boldsymbol{\theta}) = F(\boldsymbol{\phi}^*(\boldsymbol{\theta}), \boldsymbol{\theta})$ requires solving the fixed-point equation $\boldsymbol{\phi}^* = \mathcal{G}(\boldsymbol{\phi}^*; \boldsymbol{\theta})$. In the dense case, the evaluation of a single application $\mathcal{G}(\boldsymbol{\phi}, \boldsymbol{\theta})$ costs $O(d^2)$, reflecting the internal dependencies among queues.

While in a local-based case, each queue interacts only with a limited neighbors queues. Two classes of solvers may be used for obtaining ϕ^* : (i) *Direct linear solvers*, which reformulate the fixed point as a linear system in the affine case and cost $O(d^3)$. (ii) *Iterative fixed-point solvers*, such as Picard iteration or Anderson acceleration, whose per-iteration cost is $O(d^2)$, and whose total cost can be written as $C_{\text{FP}} = O(K_{\text{fp}}d^2)$.

In PG-Flow we favour iterative solvers, as they preserve sparsity, avoid matrix factorization, and lead to better scalability in large networks.

5.1 Finite Differences Applied to the Objective (FD-J)

A classical baseline approach consists of approximating $\nabla_{\boldsymbol{\theta}} J$ through centered finite differences (9): each component $\partial J / \partial \theta_j$ requires the computation of $J(\boldsymbol{\theta} + \varepsilon e_j)$ and $J(\boldsymbol{\theta} - \varepsilon e_j)$. Thus every gradient evaluation requires $2p$ steady-state solves:

$$\text{Cost}_{\text{FD-J}} = O(2p C_{\text{FP}}) = O(2p K_{\text{fp}}d^2). \quad (24)$$

Although straightforward, this approach is computationally expensive because the entire steady-state computation must be repeated for every coordinate direction. This becomes prohibitive for large-scale systems with many control parameters.

5.2 Monte-Carlo Policy Gradient

For comparison, Monte-Carlo policy-gradient methods avoid differentiating the steady state entirely. They rely instead on the identity

$$\nabla_{\boldsymbol{\theta}} J(\boldsymbol{\theta}) = \mathbb{E}[\nabla_{\boldsymbol{\theta}} \log \pi_{\boldsymbol{\theta}}(a|s) Q^{\pi}(s, a)], \quad (25)$$

whose cost is dominated by the sampling of trajectories. If N_{traj} trajectories of horizon H are required, then

$$\text{Cost}_{\text{MC}} = O(N_{\text{traj}} H). \quad (26)$$

While this estimator avoids manipulating the fixed-point equations, its variance grows with the mixing time of the queueing process. This phenomenon is particularly problematic in heavy-traffic or highly congested networks, where correlations become strong and Monte-Carlo policy gradients suffer from slow and unstable convergence. This motivates the development of deterministic, variance-free approaches such as PG-Flow.

5.3 PG-Flow with Numerical Jacobians

The PG-Flow algorithm 1 computes exact implicit gradients without perturbing the full objective, and without relying on samples. When analytical Jacobians are not available, the required matrices $\partial_{\phi} \mathcal{G}$ and $\partial_{\boldsymbol{\theta}} \mathcal{G}$ can still be recovered numerically by finite differences applied locally to \mathcal{G} , not to the full mapping $\phi^*(\boldsymbol{\theta})$. This distinction is important: the fixed-point equation is solved only *once* per iteration, after which all sensitivities are obtained from local evaluations of \mathcal{G} . Approximating the Jacobian $\partial_{\phi} \mathcal{G} \in \mathbb{R}^{d \times d}$ requires computing d^2 partial derivatives, each obtained from one

evaluation of \mathcal{G} . Since the dense cost of evaluating \mathcal{G} is $O(d^2)$, we obtain

$$\text{Cost}(\partial_\phi \mathcal{G}) = O(d^4).$$

Likewise, computing the dp entries of $\partial_\theta \mathcal{G} \in \mathbb{R}^{d \times p}$ costs

$$\text{Cost}(\partial_\theta \mathcal{G}) = O(dp d^2).$$

Once these Jacobians are available, the implicit gradient requires solving the adjoint linear system (12) whose cost is $O(d^3)$ in the dense case.

Putting all contributions together, the dominant term is the numerical evaluation of the Jacobian $\partial_\phi \mathcal{G}$, leading to

$$\text{Cost}_{\text{PG-Flow, num}} = O(d^4 + dp d^2 + d^3) = O(d^4). \quad (\text{dense}) \quad (27)$$

In locally connected networks where evaluating \mathcal{G} costs only $O(d)$, the corresponding bound reduces to

$$\text{Cost}_{\text{PG-Flow, num}} = O(d^3 + dp d + d^3) = O(d^3). \quad (\text{locally connected}) \quad (28)$$

This cost remains significantly lower than FD-J for moderate p , and benefits from the fact that only \mathcal{G} (and not the full fixed point) is perturbed.

5.4 PG-Flow with Analytical Jacobians

In many product-form queueing networks (Jackson, BCMP, G-networks, Energy-Packet Networks), both \mathcal{G} and the objective \mathcal{F} admit closed-form derivatives. In such settings, each entry of the Jacobians $\partial_\phi \mathcal{G}$ and $\partial_\theta \mathcal{G}$ can be computed in $O(1)$, with sparsity determined by the local connectivity of the network.

Let n_z denote the total number of nonzero entries across these Jacobians. In locally connected networks, $n_z = O(d)$. The overall complexity is therefore

$$\text{Cost}_{\text{PG-Flow, analytic}} = O(n_z) + O(d^3), \quad (29)$$

where the $O(d^3)$ term corresponds to solving the adjoint system. Hence, dense linear algebra dominates the iteration cost, and the Jacobian construction becomes negligible in comparison.

5.5 PG-Flow in Feed-Forward Networks

A particularly favorable situation arises when the queueing network is *feed-forward*, i.e. acyclic. In this case, the dependency structure of the flow operator is triangular, and each component \mathcal{G}_i depends only on flows from its predecessors. As a consequence, both the steady-state flows and their sensitivities propagate in a single pass. Hence, this structure has the following implications:

- the forward computation of the steady-state flows ϕ^* requires a single pass $O(d)$;

- the Jacobian $\partial_{\phi}\mathcal{G}$ contains only $O(d)$ nonzeros;
- the parameter Jacobian $\partial_{\theta}\mathcal{G}$ is block-sparse and local;
- the adjoint linear system is triangular and solves in $O(d)$ by back-substitution.

Combining these observations, the total cost of PG–Flow in a feed-forward network reduces to

$$\text{Cost}_{\text{PG–Flow, analytic, acyclic}} = O(d), \quad (30)$$

which represents the best achievable scaling: linear time per iteration. This highlights the strong link between the queuing network structure and the computational efficiency of PG–Flow. We now illustrate the practical behavior of PG–Flow on representative numerical examples in Section 6.

Table 3 Computational complexity of gradient-estimation methods for steady-state queueing networks.

Method	Gradient type	Cost / iteration
Finite differences (FD–J)	Perturb $J(\theta)$	$O(p d^2) - O(p d^3)$
PG-explicit (MC)	Stochastic PG estimator	$O(N_{\text{traj}} H)$
PG–Flow (numeric, dense)	Implicit + FD Jacobians	$O(d^4)$
PG–Flow (numeric, locally connected)	Implicit + FD Jacobians	$O(d^3)$
PG–Flow (analytic)	Implicit (closed form)	$O(n_z) + O(d^3)$
PG–Flow (analytic + acyclic)	Implicit (triangular/sparse)	$O(d)$

All PG–Flow variants that rely on exact implicit gradients (obtained either analytically or from numerically exact Jacobians) inherit the global convergence guarantees of Theorem 1 under assumptions (H1)–(H4). Acyclicity is not required for convergence: it only improves computational complexity. Identifying broader structural classes of stochastic networks (e.g., hierarchical, nearly triangular, decomposable or Nearly-Completely-Decomposable [29], with central cycles [15, 17, 30]) for which both the steady-state flow equations and the adjoint system admit sub-cubic or even linear solvers is an interesting direction for future work.

We now illustrate the practical behavior of PG–Flow on representative numerical examples in Section 6.

6 Numerical analysis

6.1 Jackson network with controllable routing matrix

We consider a three-node feed-forward Jackson network with fixed external Poisson arrivals λ_i^{ext} and two internal routing parameters. Each node corresponds to an M/M/1 queue. Jobs arrive from outside only into queue 1 with rate $\lambda_1^{\text{ext}} = 4$, while queues 2 and 3 receive no external arrivals. The service is exponential and rates are

fixed as

$$\mu = (\mu_1, \mu_2, \mu_3) = (6, 5, 7).$$

Routing is controlled at nodes 1 and 2. Upon service completion at queue 1, jobs are routed

- to queue 2 with probability $p(\theta_1)$,
- to queue 3 with probability $1 - p(\theta_1)$.

Upon service completion at queue 2, jobs are routed

- to queue 3 with probability $q(\theta_2)$,
- and leave the network with probability $1 - q(\theta_2)$.

Jobs leaving queue 3 always exit the system. The routing probability matrix is therefore expressed as:

$$P(\boldsymbol{\theta}) = \begin{bmatrix} 0 & p(\theta_1) & 1 - p(\theta_1) \\ 0 & 0 & q(\theta_2) \\ 0 & 0 & 0 \end{bmatrix}$$

The decision vector collects the two routing controls,

$$\boldsymbol{\theta} = (\theta_1, \theta_2)^\top \in \mathcal{U} = [0, 1]^2.$$

We use affine parameterizations

$$p(\theta_1) = p_0 + \theta_1, \quad q(\theta_2) = q_0 + \theta_2,$$

with nominal values $p_0 = q_0 = 0$ and bounds on $\boldsymbol{\theta}$ chosen so that $p(\theta_1), q(\theta_2) \in [0, 1]$ for all $\boldsymbol{\theta} \in \mathcal{U}$. In the numerical example below we take $\theta_1, \theta_2 \in [0, 1]$, so that $p(\theta_1) = \theta_1$, $q(\theta_2) = \theta_2$, and $p, q \in [0, 1]$. Let Λ_i denote the steady-state incoming flow at queues $i = 1, 2, 3$, and let $\boldsymbol{\phi} = (\Lambda_1, \Lambda_2, \Lambda_3)^\top$. The flow balance equations are

$$\Lambda_1 = 4, \quad \Lambda_2 = p(\theta_1) \Lambda_1, \quad \Lambda_3 = (1 - p(\theta_1)) \Lambda_1 + q(\theta_2) \Lambda_2.$$

These can be written as a fixed-point relation $\boldsymbol{\phi}^*(\boldsymbol{\theta}) = \mathcal{G}(\boldsymbol{\phi}^*(\boldsymbol{\theta}); \boldsymbol{\theta}) = A(\boldsymbol{\theta})\boldsymbol{\phi}^*(\boldsymbol{\theta}) + b(\boldsymbol{\theta})$ with $\boldsymbol{\phi} = [\phi_1, \phi_2, \phi_3]^\top$, $A(\boldsymbol{\theta}) = P(\boldsymbol{\theta})^\top$ and

$$\mathcal{G}(\boldsymbol{\phi}; \boldsymbol{\theta}) = \begin{bmatrix} \lambda_1^{\text{ext}} \\ p(\theta_1) \phi_1 \\ (1 - p(\theta_1)) \phi_1 + q(\theta_2) \phi_2 \end{bmatrix}, \quad A(\boldsymbol{\theta}) = \begin{bmatrix} 0 & 0 & 0 \\ p(\theta_1) & 0 & 0 \\ 1 - p(\theta_1) & q(\theta_2) & 0 \end{bmatrix}, \quad b(\boldsymbol{\theta}) = \begin{bmatrix} \lambda_1^{\text{ext}} \\ 0 \\ 0 \end{bmatrix}. \quad (31)$$

We aim to minimize the total mean queue length in the network. Let $\rho_i = \frac{\phi_i(\boldsymbol{\theta})}{\mu_i}$ be the load of queue i , then

$$J(\boldsymbol{\theta}) = \sum_{i=1}^3 \frac{\rho_i}{1 - \rho_i} = \sum_{i=1}^3 \frac{\Lambda_i^*(\boldsymbol{\theta})}{\mu_i - \Lambda_i^*(\boldsymbol{\theta})}. \quad (32)$$

Detailed verifications of assumptions (H1)–(H4) and the explicit first PG–Flow iteration are given in Appendix A (Jackson).

To illustrate how the PG–Flow algorithm behaves across different service-rate configurations, Figure 1 displays the cost surfaces $J(\boldsymbol{\theta})$ for the three scenarios considered (below), together with the algorithmic trajectories. Although the geometry of the landscape changes with (μ_2, μ_3) , the feasible parameter domain remains convex in all cases, in agreement with our theoretical assumptions.

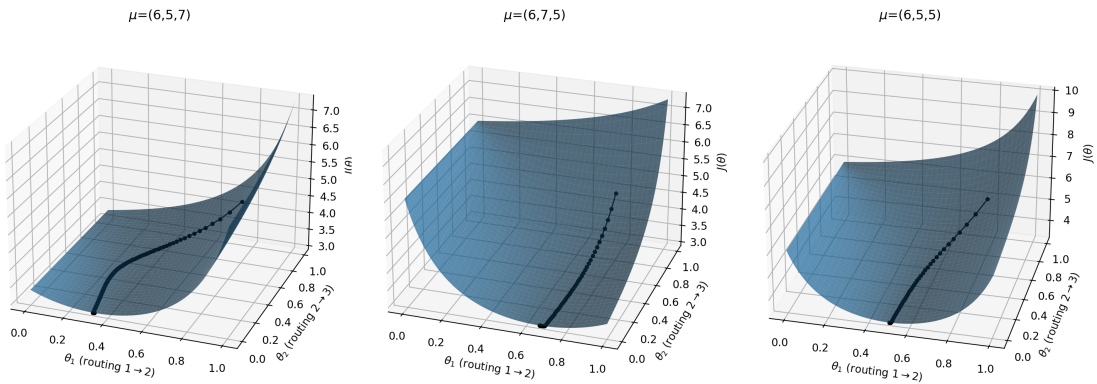


Fig. 1 Cost surfaces $J(\theta_1, \theta_2)$ for the three Jackson configurations, together with the PG-Flow trajectories (black curves).

Scenario 1: server 3 is faster.

In this experiment (the one detailed in Appendix A), we considered a Jackson network with service rates $\mu = (\mu_1, \mu_2, \mu_3) = (6, 5, 7)$, where server 3 is faster than server 2. The PG-Flow algorithm yields the optimal parameters

$$\boldsymbol{\theta}^* \approx (0.3313, 0), \quad \boldsymbol{\phi}^* \approx (4, 1.33, 2.67), \quad J(\boldsymbol{\theta}^*) \approx 2.979.$$

Thus, the optimal policy routes only about one third of the input flow through queue 2, while setting $q^* = 0$ to avoid sending customers from queue 2 to the slower queue 3. Since $\mu_3 > \mu_2$, the optimal routing chooses predominantly the faster path $1 \rightarrow 3$ and avoids the slower path $1 \rightarrow 2 \rightarrow 3$.

Scenario 2: server 2 becomes faster.

To analyze how the optimal routing changes when service capacities are modified, we consider the reversed situation

$$\mu = (6, 7, 5),$$

where server 2 is now faster than server 3. The PG-Flow algorithm converges to

$$\boldsymbol{\theta}^* \approx (0.6688, 0), \quad \boldsymbol{\phi}^* \approx (4, 2.68, 1.32), \quad J(\boldsymbol{\theta}^*) \approx 2.979.$$

The optimal policy therefore *switches side*: a large fraction of the incoming flow is now routed to queue 2, and only a small residual flow enters queue 3. As in Scenario 1, the algorithm finds $q^* = 0$, meaning that customers leave the system directly after queue 2, which is now the fastest internal server. Thus the optimized policy always favors routing through the fastest available server.

Scenario 3: balanced internal servers.

Finally, we consider a configuration where the two internal servers have equal service rates,

$$\mu = (6, 5, 5).$$

In this case PG-Flow converges to

$$\boldsymbol{\theta}^* \approx (0.5013, 0), \quad \boldsymbol{\phi}^* \approx (4, 2.01, 1.99), \quad J(\boldsymbol{\theta}^*) \approx 3.333.$$

Since $\mu_2 = \mu_3$, the optimal routing splits the flow almost equally between queues 2 and 3. However, because both servers are slower than in Scenarios 1–2, the global performance is significantly worse: $J(\boldsymbol{\theta}^*)$ is strictly larger.

Overall comparison. Scenarios 1 and 2 achieve similar and significantly lower optimal costs ($J(\boldsymbol{\theta}^*) \approx 2.98$), each by directing the majority of the flow toward the fastest internal server. Scenario 3, where the internal servers are slower and balanced, yields a noticeably higher cost ($J(\boldsymbol{\theta}^*) \approx 3.33$). Hence the most favorable configuration is obtained when a single internal server is sufficiently fast, allowing the optimizer to route most of the flow through it. Another observation is that in all three scenarios, the PG-Flow solution satisfies either $p^* = 0$ or $q^* = 0$. In these cases, the steady-state flows obey the conservation identity $\Lambda_2 + \Lambda_3 = \Lambda_1$. This matches the analytical expression

$$\Lambda_1 = 4, \quad \Lambda_2 = 4p, \quad \Lambda_3 = 4(1 - p + pq) \implies \Lambda_2 + \Lambda_3 = 4 + 4pq,$$

which reduces to $\Lambda_2 + \Lambda_3 = \Lambda_1$ when $p = 0$ or $q = 0$. Thus, the conservation pattern observed numerically is fully consistent with the model's flow equations.

6.2 Energy Packet Network with controllable energy arrivals

In this second application, we consider the Energy Packet Network (EPN) composed of N interconnected nodes presented in [27]. Each node $i \in \{1, \dots, N\}$ contains:

- an infinite Data Packet (DP) queue with external Poisson arrivals of rate λ_i^{ext} ;
- an infinite Energy Packet (EP) queue receiving EPs at a *controllable* Poisson rate $\alpha_i = \alpha_i(\boldsymbol{\theta})$;
- a DP service is triggered by the EP queue: at each service event, one EP triggers the departure of a single DP from the DP queue (if a DP is available). If no EPs are available, DPs wait in the DP queue until the next EP arrival. After service, the EP is consumed and the DP is forwarded to another queue according to the routing matrix P .
- an energy leakage mechanism in the EP queue where EPs disappear at exponential rate γ_i (representing the physical energy leakage that may occur in IoT batteries).

We restrict ourselves to the Coxian case with one phase $K = 1$ (i.e., exponential EP service times). The steady-state consumption rate of EPs at node i is:

$$\beta_i(\boldsymbol{\theta}) = \frac{\alpha_i(\boldsymbol{\theta})}{\gamma_i + \mu_i}, \quad (33)$$

where μ_i is the exponential EP service parameter. Thus, the EP flow depends affinely on the control vector $\boldsymbol{\theta}$.

Routing of data packets. Only DP flows are routed between nodes. Each DP served at node i is forwarded to node j with fixed probability $P_{i,j}$ or leaves the network with probability $d_i = 1 - \sum_{j=1}^N P_{i,j}$. Routing probabilities are *not* controlled in this experiment. Instead, the control acts solely on the EP arrival rates $\alpha_i(\boldsymbol{\theta})$. This highlights the versatility of PG-Flow, which can optimize arbitrary differentiable steady-state parameters (routing, service rates, or energy input levels) without altering the mathematical structure.

Steady-state flow equations. Let $\rho_i(\boldsymbol{\theta})$ denote the DP utilization at node i . Since the effective DP service rate is $\mu_i \beta_i(\boldsymbol{\theta})$, the DP balance equations (special case $K = 1$ of [27]) are:

$$\rho_i(\boldsymbol{\theta}) = \frac{\lambda_i^{\text{ext}} + \sum_{j=1}^N \mu_j \rho_j(\boldsymbol{\theta}) \beta_j(\boldsymbol{\theta}) P_{j,i}}{\mu_i \beta_i(\boldsymbol{\theta})}, \quad i = 1, \dots, N. \quad (34)$$

Multiplying (34) by $\mu_i \beta_i(\boldsymbol{\theta})$ yields:

$$\rho_i(\boldsymbol{\theta}) \mu_i \beta_i(\boldsymbol{\theta}) = \lambda_i^{\text{ext}} + \sum_{j=1}^N \mu_j \rho_j(\boldsymbol{\theta}) \beta_j(\boldsymbol{\theta}) P_{j,i}. \quad (35)$$

Define the DP flow:

$$\phi_i(\boldsymbol{\theta}) := \rho_i(\boldsymbol{\theta}) \mu_i \beta_i(\boldsymbol{\theta}). \quad (36)$$

Then the DP equations reduce to the classical Jackson flow equations:

$$\phi_i(\boldsymbol{\theta}) = \lambda_i^{\text{ext}} + \sum_{j=1}^N \phi_j(\boldsymbol{\theta}) P_{j,i}. \quad (37)$$

Hence, DP flows satisfy the linear fixed-point system:

$$\phi^*(\boldsymbol{\theta}) = A\phi^*(\boldsymbol{\theta}) + b, \quad (38)$$

where $A = P^\top$ and $b = (\lambda_1^{\text{ext}}, \dots, \lambda_N^{\text{ext}})^\top$. Importantly, since routing is fixed, A and b do *not* depend on $\boldsymbol{\theta}$. All dependence on $\boldsymbol{\theta}$ arises through the EP flows $\beta_i(\boldsymbol{\theta})$.

Performance objective and QoS–Energy trade-off. Two antagonistic performance metrics arise naturally in EPNs:

- **DP queueing delay (Quality of Service):**

$$D(\boldsymbol{\theta}) = \sum_{i=1}^N \frac{\rho_i(\boldsymbol{\theta})}{1 - \rho_i(\boldsymbol{\theta})} = \sum_{i=1}^N \frac{\phi_i(\boldsymbol{\theta})}{\mu_i \beta_i(\boldsymbol{\theta}) - \phi_i(\boldsymbol{\theta})},$$

where the expression corresponds to an $M/M/1$ queue with service rate $\mu_i \beta_i(\boldsymbol{\theta})$. Increasing $\alpha_i(\boldsymbol{\theta})$ increases $\beta_i(\boldsymbol{\theta})$ and hence reduces delay.

- **EP leakage (energy waste):**

$$L(\boldsymbol{\theta}) = \sum_{i=1}^N \gamma_i \beta_i(\boldsymbol{\theta}) = \sum_{i=1}^N \gamma_i \frac{\alpha_i(\boldsymbol{\theta})}{\gamma_i + \mu_i}.$$

Increasing α_i increases the energy waste.

These metrics are structurally conflicting: more incoming energy improves QoS but increases the system's energy consumption. We consider the scalarized objective:

$$J(\boldsymbol{\theta}) = w_1 D(\boldsymbol{\theta}) + w_2 L(\boldsymbol{\theta}), \quad w_1, w_2 \geq 0, \quad (39)$$

which expresses explicitly the QoS–Energy compromise.

Detailed verifications of assumptions (H1)–(H4) and the explicit first PG–Flow iteration are given in Appendix B (EPN). Now, we present the following results.

Starting from the uniform allocation $\boldsymbol{\theta}^{(0)} = (5, 5, 5, 5, 5)$ with total budget $B_{\max} = 25$, PG–Flow converges after about 120 iterations to an energy allocation

$$\boldsymbol{\theta}^* \approx (4.88, 4.80, 5.98, 2.91, 6.44), \quad \sum_{i=1}^5 \theta_i^* = 25.$$

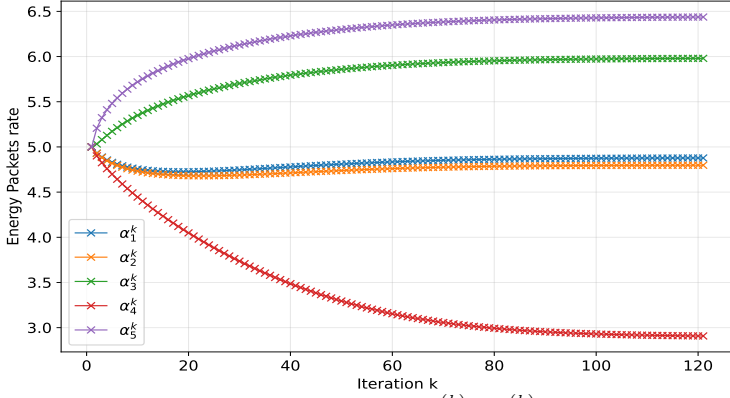


Fig. 2 Evolution of the energy-allocation parameters $\alpha_i^{(k)} = \theta_i^{(k)}$ over the PG-Flow iterations.

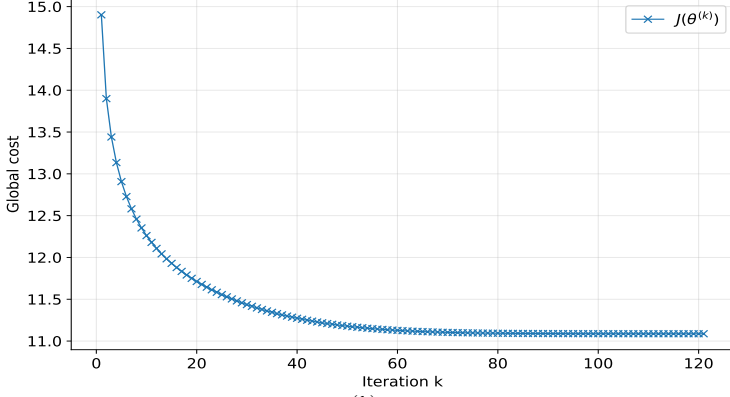


Fig. 3 Monotone decrease of the objective $J(\theta^{(k)})$ along PG-Flow iterations.

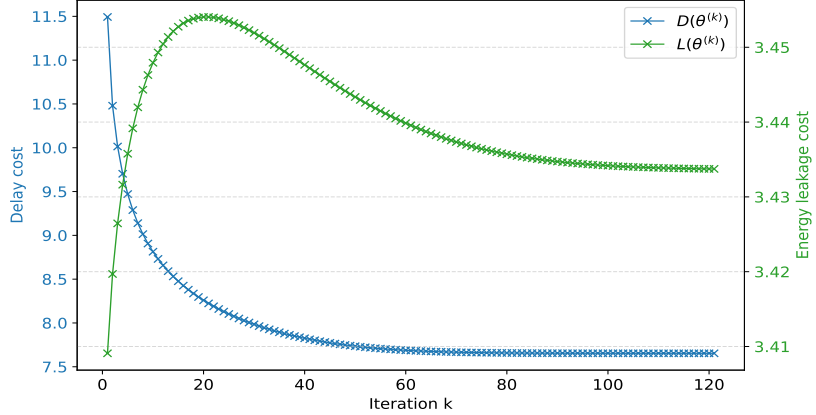


Fig. 4 Decomposition of the objective into delay $D(\theta^{(k)})$ and leakage $L(\theta^{(k)})$ components.

The corresponding EP loads are

$$\beta^* \approx (0.44, 0.44, 1.00, 0.48, 1.07),$$

and the steady-state DP flows remain

$$\phi^* \approx (2.64, 2.58, 3.19, 1.27, 3.48),$$

as determined by the Jackson flow equations. Hence nodes 3 and 5 carry the largest DP loads and are structurally central in the network (in particular through the cycles involving nodes 1–3–5), while node 4 carries a comparatively small flow. It is therefore natural, from the point of view of delay minimization, that PG–Flow learns to concentrate energy on nodes 3 and 5, to a lesser extent on nodes 1 and 2, and to allocate very little energy to node 4. The limiting allocation θ^* can thus be interpreted as a principled way of “feeding” the main bottlenecks of the network under a global budget constraint.

Figure 2 illustrates the evolution of the five components $\alpha_i^{(k)} = \theta_i^{(k)}$ along the iterations. Starting from the uniform vector, the parameters quickly separate and then stabilize, with the clear ordering

$$\theta_5^* \gtrsim \theta_3^* > \theta_1^* \approx \theta_2^* \gg \theta_4^*.$$

This behavior is fully consistent with the structure of the steady-state DP flows: the nodes that process the largest amount of traffic (3 and 5) end up receiving most of the energy, whereas node 4, which sees only a modest flow and primarily acts as a transient node towards node 5, is assigned a very small share of the budget. The trajectories in Figure 2 can therefore be read as the progressive redistribution of energy away from lightly utilized nodes and towards the main DP bottlenecks. The evolution of the objective $J(\theta^{(k)})$ is reported in Figure 3. Initially, we have

$$J(\theta^{(0)}) = D(\theta^{(0)}) + L(\theta^{(0)}) \approx 11.49 + 3.41 \approx 14.90,$$

while at the final iterate

$$J(\theta^*) \approx 11.09 \quad \text{with} \quad D(\theta^*) \approx 7.65, \quad L(\theta^*) \approx 3.43.$$

The curve $k \mapsto J(\theta^{(k)})$ decreases monotonically and shows a typical pattern for gradient-based schemes: a fast decrease during the first few tens of iterations, followed by a refinement regime in which the objective approaches its limiting value more slowly. The small relative improvement observed at the final iterations is consistent with PG–Flow having reached a point close to a global minimum.

To better understand the underlying trade-off, Figure 4 displays separately the delay component $D(\theta^{(k)})$ and the energy leakage $L(\theta^{(k)})$. At the beginning of the trajectory, D decreases sharply, while L increases moderately: PG–Flow first exploits the available budget more aggressively, pushing energy towards the heavily loaded nodes in order to dissipate congestion and reduce queueing delay. Once the main delay reduction has been achieved, the curve $D(\theta^{(k)})$ flattens, and subsequent iterations mostly adjust the allocation to re-balance leakage and delay. In this later phase, $L(\theta^{(k)})$ slightly decreases again, while $D(\theta^{(k)})$ remains essentially stable, leading to a final allocation that realises a sensible compromise between queueing performance

and energy leakage. Overall, Figures 2–4 provide a coherent behavior: starting from a uniform allocation, PG-Flow reassigns energy to the critical nodes 3 and 5, yields a substantial reduction of the delay component, and settles on a stable operating point where the total cost J is the closest to its optimal value.

6.3 Performance evaluation of the algorithms

In this section, we compare the algorithms introduced in Section 5. (i) **FD-J** denotes the baseline approach, where $\nabla_{\theta} J$ is approximated using finite-difference gradients. (ii) **PG-num** refers to the Policy-Gradient Flow method proposed in this work, but relying exclusively on numerical solvers for the flow fixed point, the adjoint system, and the Jacobian of \mathcal{G} . (iii) **PG-analytic** corresponds to the optimized version of PG-Flow specialized to forward (i.e., acyclic) queueing networks, where all derivatives admit closed-form expressions. (iv) **PPO** (Proximal Policy Optimization) represents a simulation-based algorithm relying on Monte Carlo trajectory sampling. PPO introduced by Schulman et al. (2017) in [31], is a policy-gradient method specifically designed to address the stability issues of classical Actor-Critic and REINFORCE algorithms. Instead of applying potentially large parameter updates—which often lead to high-variance gradients and poor learning stability—PPO constrains successive policies to remain close to each other through a clipped surrogate objective. This results in significantly more stable and monotonic policy improvement while retaining the simplicity and sample-efficiency of first-order methods. We include PPO in our comparison because it is widely regarded as one of the most reliable simulation-based policy-gradient algorithms in reinforcement learning: it is substantially more robust to hyper-parameters, less sensitive to noise, and typically achieves smoother convergence than standard Actor-Critic (A2C/A3C) methods [31]. For each method, we report, in Table 4 and 5, the final global cost $J(\theta)$, the number of iterations required to reach convergence (or a prescribed precision ε), and the total execution time (CPU time).

Network generation. For the synthetic experiments reported in tables below, we generate random Jackson networks structured as directed acyclic graphs (DAGs), in the spirit of the construction described in Subsection 6.1. This design enables a fair comparison of all optimization methods discussed in Section 5.

Given the number of queues d and the number of controllable routing links p , we construct a forward DAG in which each node i only routes flow to nodes $j > i$. External arrivals occur only at node 0, with rate $\lambda_0^{\text{ext}} = 4$. Service rates alternate between “slow” and “fast” servers, i.e., $\mu_i \in \{8, 12\}$ according to the parity of i . Among the nodes $\{1, \dots, d-2\}$, a subset of size p is randomly selected as controllable branching nodes. At each such node i , we create two outgoing arcs: a “slow” arc to $i+1$ and a “fast” arc to a randomly chosen successor $j > i+1$. Their routing probabilities are parametrized by a control variable θ_k , namely $P(i \rightarrow i+1) = 1 - \theta_k$ and $P(i \rightarrow j) = \theta_k$. All remaining nodes are non-controllable and route flow according to fixed probabilities: a random value $x \in (0.2, 0.8)$ determines $P(i \rightarrow i+1) = x$ and $P(i \rightarrow j) = 1 - x$ for a randomly selected $j > i+1$. Node $d-1$ has a single fixed successor d , and node d has no outgoing arcs, meaning that all departures from d immediately leave the network.

Openness. This construction guarantees that the network is open for all $\theta \in \mathcal{U}$ (with $\mathcal{U} = [0, 1]^p$). That is, for every $i < d$, every queue admits a directed path

$i \rightarrow i+1 \rightarrow i+2 \rightarrow \dots \rightarrow d$ with strictly positive probability. Thus every job exits the system in a finite number of steps. Finally, the presence of fixed (non-controllable) routing links plays an important role: they act as *structural constraints* that limit the action space and make the resulting optimization problem more realistic and challenging.

Stability. In all generated instances, stability is guaranteed for any $\boldsymbol{\theta} \in \mathcal{U}$. Since external arrivals occur only at node 1 with rate 4 and the routing graph is a forward DAG. Hence the effective arrival rate satisfies $\phi_i^*(\boldsymbol{\theta}) \leq 4$ for all i . With service rates $\mu_i \in \{8, 12\}$, we have $\rho_i(\boldsymbol{\theta}) = \frac{\phi_i^*(\boldsymbol{\theta})}{\mu_i} \leq \frac{4}{8} < 1$. Hence the network is stable for all admissible parameters.

Other hypothesis verifications (H3) and (H4) follow the same arguments as in Appendix A.

Objective. We fixed the optimized quantity as the total mean number of tasks in the system, i.e., the standard Jackson-network cost $J(\boldsymbol{\theta})$ defined in (32).

Hyper-parameter setting. We fixed the same stopping condition for all optimization methods (FD–J, PG–num and PG–analytic). At iteration k , the algorithm stops whenever

$$\frac{|J(\boldsymbol{\theta}_k) - J(\boldsymbol{\theta}_{k-1})|}{\max(1, |J(\boldsymbol{\theta}_{k-1})|)} \leq \epsilon_J \quad \text{or} \quad \|\nabla J(\boldsymbol{\theta}_k)\|_2 \leq \epsilon_\nabla,$$

where the first test monitors the *relative* improvement of the objective, and the second corresponds to a first-order optimality condition. The tolerances were chosen so as to ensure reliable convergence without performing unnecessary iterations: we use $\epsilon_J = 10^{-6}$, $\epsilon_\nabla = 10^{-4}$, and `max_Iter` = 500. Additional internal tolerances are required for implicit-differentiation methods. In PG–num, the steady-state flows $\phi^*(\boldsymbol{\theta})$ are computed by Anderson acceleration with a fixed-point tolerance $\epsilon_\phi = 10^{-10}$, and all derivatives ∂_ϕ and $\partial_{\boldsymbol{\theta}}$ are approximated by finite differences using a step $\epsilon_\partial = 10^{-8}$. For FD–J, the finite-difference approximation is applied directly to the full objective J , using the same internal finite-difference step ϵ_∂ . For all methods, the parameters are updated through a projected gradient step with a constant step-size $\eta = 0.05$.

For the Monte-Carlo simulation based baseline (PPO), the hyper-parameters must be chosen with care to obtain stable gradients and a reasonable variance–bias trade-off. In all experiments, we fix the number of policy updates to $n_{\text{iter}} = 50$, and each update is based on a batch of $N_{\text{traj}} = 100$ simulated trajectories. Each trajectory is generated over a finite time horizon $H \in \{50, 100\}$ (refer to Table 4). For each batch of trajectories, the PPO objective is optimized for $n_{\text{epochs}} = 4$ epochs using the Adam optimizer with learning rate 10^{-2} and clipping parameter $\varepsilon_{\text{clip}} = 0.2$. These values provided a good balance between computational cost and stability, while avoiding the high variance issues typically observed when using longer horizons or smaller batches.

Analysis of results. Table 4 compares the four optimization approaches on small and medium-sized Jackson DAGs. The PG-analytic method provides a useful reference point, as it computes exact gradients with a linear-time complexity in acyclic networks (Equation (30)). Its execution time remains very low across all problem sizes, and it consistently satisfies the stopping criterion. The PG–num and FD–J methods also produce accurate solutions, especially for small networks, but their reliance

Table 4 Performance comparison for small and medium-scale Jackson DAGs. Where d the number of queues and p the number of control parameters.

d	p	Method	$J(\theta^*)$	Iterations	Exec. time (s)
10	3	PG-analytic	2.4737	106	0.006
		PG-num	2.4737	106	0.396
		FD-J	2.4737	106	0.263
		PPO ($H=50$)	2.5150	50	42.24
50	20	PG-analytic	5.3015	346	0.188
		PG-num	5.5722	500	15.66
		FD-J	5.5811	500	33.49
		PPO ($H=50$)	5.4766	50	117.19
100	40	PG-analytic	4.9482	263	0.237
		PG-num	5.4432	500	160.50
		FD-J	5.0723	500	1399.61
		PPO ($H=100$)	5.2886	50	174.85

Table 5 Scalability of the PG-analytic method on large Jackson DAGs. Where d the number of queues and p the number of control parameters.

d	p	$J(\theta^*)$	Iterations	Exec. time (s)
5 000	2000	5.64	707	29.10
	4000	4.69	202	9.28
10 000	3000	6.96	1388	172.82
	9000	4.73	724	95.55
50 000	20 000	7.07	1318	1252.43
	40 000	5.32	130	262.05
100 000	50 000	7.32	1330	1022.68
	80 000	4.98	111	429.79
200 000	150 000	5.91	355	1739.83

on finite-difference perturbations introduces numerical sensitivity as d grows. This effect is visible in the objective values for $d = 50$ and $d = 100$, where both methods reach the maximum iteration (500 iterations) without meeting the targeted precision $\epsilon_J = 10^{-5}$. Their execution times align with the theoretical complexities discussed in Section 5, which increases computational cost for larger dimensions. The PPO method produces approximate solutions across all settings and returns objective values of the same general order as the finite-difference approaches. Its performance depends on several hyper-parameters, such as the horizon length H and the number of sampled trajectories N_{traj} , and each iteration requires evaluating approximately $N_{\text{traj}} \times H$ simulated transitions. For the small and medium networks considered here, the resulting execution time remains reasonable, but PPO becomes substantially slower in larger systems, as longer horizons are typically required for trajectories to reach the steady-state behavior of the queues. For instance, a simulation of $d = 500$ and $p = 300$ yields 4505.8 seconds (with $H = 200$ and $N_{\text{traj}} = 100$) with $J(\theta) = 4.56$, while PG-analytic converges in 0.45 seconds achieving $J(\theta) = 4.52$. Overall, PPO provides meaningful

approximate solutions, while PG-analytic achieves the most favorable balance between accuracy, convergence, and computational efficiency.

Given the promising results of PG-analytic in Table 4, we further investigate its scalability in Table 5. The execution times grow approximately linearly with d , in accordance with the per-iteration complexity of Equation (30) in the acyclic setting. This behavior confirms that PG-analytic remains suitable for problems involving tens of thousands of queues and beyond.

A second observation concerns the influence of the number of control parameters p . When p is relatively small (compared to d), such as $d = 100,000$ and $p = 50,000$ (or even lower), each iteration is computationally inexpensive, but the optimization typically requires more iterations to reach the stopping criterion. This behavior is expected: fixing a large subset of non-controlled routing parameters reduces the dimensionality of the control space and therefore limits the flexibility of the optimization process. With fewer degrees of possibilities, additional iterations are needed to compensate for these structural constraints.

Conversely, when p is larger—for example $p = 80,000$ for $d = 100,000$ —the optimization benefits from a richer parametrization and converges in substantially fewer iterations, despite a slightly higher per-iteration computation time. A related observation is that the objective value $J(\boldsymbol{\theta}^*)$ decreases as p increases. This is consistent with the fact that enlarging the controllable parameter space provides more opportunities to reduce the total cost, whereas fixed (non-controllable) parameters effectively act as constraints. Overall, these results confirm both the scalability and the practical robustness of the PG-analytic approach, while highlighting the important interplay between network size and policy parametrization in large-scale optimization.

Experiments were conducted on a laptop equipped with 10 CPU cores (8 cores at 3.2 GHz peak frequency and 2 cores at 2.0 GHz), and 16 GB of RAM.

7 Conclusion

We introduced PG-Flow, a deterministic policy-gradient framework for steady-state optimization in geometric product-form queueing networks. By expressing classical performance metrics in terms of local steady-state flows, the method leverages the fixed-point structure of product-form models and computes exact policy gradients via implicit differentiation and a local adjoint system. We established global convergence under affine flow operators and natural convexity assumptions, and identified acyclic network structures that enable linear-time implementations. Numerical experiments on routing control in Jackson networks and on energy-arrival control in Energy Packet Networks demonstrated the effectiveness and scalability of the approach.

Several directions for future work arise naturally. One avenue is to extend PG-Flow beyond geometric product-form networks, either by considering richer steady-state parametrizations or by incorporating approximate flow representations. Another promising direction is the integration of PG-Flow within adaptive or online control architectures, combining deterministic gradients with real-time measurements. Finally, exploiting sparsity, decomposability, or hierarchical structures

may allow further reductions in computational cost. We hope that PG-Flow contributes to strengthening the interface between analytical queueing theory and modern gradient-based methods for steady-state control.

References

- [1] Jackson, J.R.: Networks of waiting lines. *Operations Research* **5**(4), 518–521 (1957) <https://doi.org/10.1287/opre.5.4.518>
- [2] Forest Baskett, R.R.M. K. Mani Chandy, Palacios, F.G.: Open, closed, and mixed networks of queues with different classes of customers. *Journal of the ACM* **22**(2), 248–260 (1975)
- [3] Gelenbe, E.: Product-form queueing networks with negative and positive customers. *Journal of Applied Probability* **28**(3), 656–663 (1991) <https://doi.org/10.2307/3214499>
- [4] Gelenbe, E.: G-networks by triggered customer movement. *Journal of Applied Probability* **30**(3), 742–748 (1993) <https://doi.org/10.2307/3214781>
- [5] Boucherie, R.J., Dijk, N.M.: *Queueing Networks: A Fundamental Approach*. Springer, New York (2010). <https://doi.org/10.1007/978-1-4419-6472-4>
- [6] Comte, C., Dorsman, J.-P.: Pass-and-swap queues. *Queueing Systems* **98**, 275–331 (2021) <https://doi.org/10.1007/s11134-021-09700-3>
- [7] Gelenbe, E., Fourneau, J.-M.: G-networks with resets. *Performance Evaluation* **49**(1), 179–191 (2002) [https://doi.org/10.1016/S0166-5316\(02\)00127-X](https://doi.org/10.1016/S0166-5316(02)00127-X)
- [8] Gelenbe, E.: Energy packet networks: adaptive energy management for the cloud. In: *Proceedings of the 2nd International Workshop on Cloud Computing Platforms. CloudCP '12*. Association for Computing Machinery, New York, NY, USA (2012). <https://doi.org/10.1145/2168697.2168698>
- [9] Gelenbe, E., Ceran, E.T.: Energy packet networks with energy harvesting. *IEEE Access* **4**, 1321–1331 (2016) <https://doi.org/10.1109/ACCESS.2016.2545340>
- [10] Puterman, M.L.: *Markov Decision Processes: Discrete Stochastic Dynamic Programming*. Wiley, New York, USA (1994)
- [11] Bertsekas, D.P.: *Nonlinear Programming*, 2nd edn. Athena Scientific, Athena Scientific, Belmont, MA (1999)
- [12] Dietterich, T.G.: Hierarchical reinforcement learning with the maxq value function decomposition. *Journal of Artificial Intelligence Research* **13** (2000) <https://doi.org/10.1613/jair.639>

- [13] Barto, A.G., Mahadevan, S.: Recent advances in hierarchical reinforcement learning. *Discrete Event Dynamic Systems* **13**(4) (2003) <https://doi.org/10.1023/A:1025696116075>
- [14] Koller, D., Parr, R.: Computing factored value functions for policies in structured mdps. In: Proc. 16th International Joint Conference on Artificial Intelligence (IJCAI) (1999). <https://doi.org/10.5555/646307.687921>
- [15] Ait El Mahjoub, Y., Fourneau, J.-M.: A slot-based energy storage decision-making approach for optimal off-grid telecommunication operator. *Computer Communications* **242**, 108273 (2025) <https://doi.org/10.1016/j.comcom.2025.108273>
- [16] Ait El Mahjoub, Y., Fourneau, J.-M.: Finding the optimal policy to provide energy for an off-grid telecommunication operator. In: 2024 20th International Conference on Wireless and Mobile Computing, Networking and Communications (WiMob), pp. 713–720 (2024). <https://doi.org/10.1109/WiMob61911.2024.10770514>
- [17] Ait El Mahjoub, Y., Fourneau, J.-M., Alouah, S.: Efficient solving of large single input superstate decomposable markovian decision process. *arXiv e-prints*: (2025) <https://doi.org/10.48550/arXiv.2508.00816>
- [18] Sutton, R.S., McAllester, D., Singh, S., Mansour, Y.: Policy gradient methods for reinforcement learning with function approximation. In: *Advances in Neural Information Processing Systems*, vol. 12. MIT Press, Cambridge, MA (1999)
- [19] Konda, V., Tsitsiklis, J.: Actor-critic algorithms. In: Solla, S., Leen, T., Müller, K. (eds.) *Advances in Neural Information Processing Systems*, vol. 12. MIT Press, Cambridge, MA (1999)
- [20] Domke, J.: Generic methods for optimization-based modeling. In: Lawrence, N.D., Girolami, M. (eds.) *Proceedings of the Fifteenth International Conference on Artificial Intelligence and Statistics*, vol. 22, pp. 318–326. PMLR, La Palma, Canary Islands (2012)
- [21] Gould, S., Hartley, R., Campbell, D.: Deep declarative networks. *IEEE Transactions on Pattern Analysis and Machine Intelligence* **44**(8), 3988–4004 (2022) <https://doi.org/10.1109/TPAMI.2021.3059462>
- [22] Sanders, J., Borst, S.C., Leeuwaarden, J.S.H.: Online optimization of product-form networks. In: 6th International ICST Conference on Performance Evaluation Methodologies and Tools, pp. 21–30 (2012). <https://doi.org/10.4108/valuetools.2012.250261>
- [23] Comte, C., Jonckheere, M., Sanders, J., Senen-Cerda, A.: Score-aware policy-gradient methods and performance guarantees using local lyapunov conditions:

Applications to product-form stochastic networks and queueing systems. *Journal of Machine Learning Research* (2025). also arXiv:2312.02804

- [24] Neely, M.J.: Stochastic Network Optimization with Application to Communication and Queueing Systems. *Synthesis Lectures on Learning, Networks, and Algorithms*. Springer, University of Southern California (2010). <https://doi.org/10.1007/978-3-031-79995-2>
- [25] Tsai, E.R., Demirtas, D., Tintu, A.N., de Jonge, R., de Rijke, Y.B., Boucherie, R.J.: Design of fork-join networks of first-in-first-out and infinite-server queues applied to clinical chemistry laboratories. *European Journal of Operational Research* **310**(3), 1101–1117 (2023) <https://doi.org/10.1016/j.ejor.2023.04.003>
- [26] Fourneau, J.-M., Ait El Mahjoub, Y.: Processor sharing G-queues with inert customers and catastrophes: A model for server aging and rejuvenation. *Probability in the Engineering and Informational Sciences* **31**(4), 420–435 (2017) <https://doi.org/10.1017/S0269964817000092>
- [27] Ait El Mahjoub, Y., Fourneau, J.-M., Castel-Taleb, H.: Energy packet networks with general service time distribution. In: 28th International Symposium on Modeling, Analysis, and Simulation of Computer and Telecommunication Systems (MASCOTS), pp. 1–8 (2020). <https://doi.org/10.1109/MASCOTS50786.2020.9285965>
- [28] Boyd, S., Vandenberghe, L.: Convex Optimization. Cambridge University Press, Cambridge (2004)
- [29] Stewart, W.J.: Introduction to the Numerical Solution of Markov Chains. Princeton University Press, Princeton, NJ (1994)
- [30] Robertazzi, T.G.: Computer Networks and Systems: Queueing Theory and Performance Evaluation. Springer, New York, NY (1990). <https://doi.org/10.1007/978-1-4684-0385-5>
- [31] Schulman, J., Wolski, F., Dharwal, P., Radford, A., Klimov, O.: Proximal policy optimization algorithms. ArXiv e-prints (2017) <https://doi.org/https://arxiv.org/pdf/1707.06347.pdf>

A Appendix: Jackson Network

Verification of the PG–Flow assumptions

We verify that this network satisfies the structural conditions of Section 4.

(H1) Convex and compact domain.

We consider the rectangular parameter domain

$$\mathcal{U} = [\theta_{1,\min}, \theta_{1,\max}] \times [\theta_{2,\min}, \theta_{2,\max}] = [0, 1] \times [0, 1],$$

which is nonempty, convex, and compact. The routing probabilities are $p(\theta_1) = \theta_1$, $q(\theta_2) = \theta_2$, and therefore lie in $[0, 1]$ for all $\boldsymbol{\theta} \in \mathcal{U}$. The steady-state flows are

$$\Lambda_1 = \lambda_1^{\text{ext}}, \quad \Lambda_2 = \lambda_1^{\text{ext}} p(\theta_1), \quad \Lambda_3 = \lambda_1^{\text{ext}} (1 - p(\theta_1) + q(\theta_2)p(\theta_1)), \quad (40)$$

which satisfy

$$0 \leq \Lambda_2 \leq \lambda_1^{\text{ext}}, \quad 0 \leq \Lambda_3 \leq \lambda_1^{\text{ext}}.$$

Since $\lambda_1^{\text{ext}} = 4$ then $\Lambda_i < \mu_i = (6, 5, 7)$ for all $\boldsymbol{\theta} \in \mathcal{U}$, the network is stable throughout \mathcal{U} . Hence (H1) holds.

(H2) Openness.

By definition, the dependency network $A(\boldsymbol{\theta})$ is feed-forward, hence for every queue there is a path to a departure queue. This structure holds for every $\boldsymbol{\theta} \in \mathcal{U}$.

(H3) Monotonicity of the steady-state flows.

In this acyclic Jackson network, the steady-state flows admit the closed-form expressions (40) on \mathcal{U} , the routing probabilities $p(\theta_1) = \theta_1$, $q(\theta_2) = \theta_2$ are coordinate-wise non-decreasing. Differentiating the steady-state flows yields

$$\frac{\partial \Lambda_2}{\partial p} = 4 \geq 0, \quad \frac{\partial \Lambda_3}{\partial p} = 4 q(\theta_2) \geq 0, \quad \frac{\partial \Lambda_3}{\partial q} = 4 p(\theta_1) \geq 0.$$

Hence, for any $\boldsymbol{\theta} \leq \boldsymbol{\theta}'$ (component-wise), $\Lambda_i(\boldsymbol{\theta}) \leq \Lambda_i(\boldsymbol{\theta}')$ for $i \in \{1, 2, 3\}$. Thus the steady-state flow vector $\boldsymbol{\phi}^*(\boldsymbol{\theta})$ is coordinate-wise non-decreasing in the control parameters, and (H3) holds.

(H4) Convex and monotone local rewards.

Each queue $i \in \{1, 2, 3\}$ has local reward $r_i(x) = \frac{x}{\mu_i - x}$, $x \in [0, \mu_i]$, which is convex and strictly increasing. The steady-state objective can be written as $J(\boldsymbol{\theta}) = \sum_{i=1}^3 r_i(\Lambda_i^*(\boldsymbol{\theta}))$. Since each r_i is convex and non-decreasing and each $\Lambda_i^*(\boldsymbol{\theta})$ is coordinate-wise non-decreasing by (H3), the composition $r_i(\Lambda_i^*(\boldsymbol{\theta}))$ is convex on \mathcal{U} . Therefore (H4) holds.

In conclusion, all assumptions (H1)–(H4) of Theorem 1 are satisfied for this two-parameter Jackson network. In the next subsection, we provide details of the first iteration of PG-flow.

First PG-Flow iteration

We initiate PG-flow control parameters with $\boldsymbol{\theta}_0 = (0.8, 0.8)$. hence

$$p_0 = p(\theta_{1,0}) = 0.8, \quad q_0 = q(\theta_{2,0}) = 0.8.$$

1. Flow equations.

At θ_0 , the steady-state flows are

$$\Lambda_1^{(0)} = 4, \quad \Lambda_2^{(0)} = 4p_0 = 3.2, \quad \Lambda_3^{(0)} = 4(1 - p_0 + q_0 p_0) = 3.36.$$

Thus

$$\phi^{(0)} = \begin{bmatrix} 4 \\ 3.2 \\ 3.36 \end{bmatrix}.$$

2. Objective value.

The initial cost is

$$J(\theta_0) = \frac{4}{6-4} + \frac{3.2}{5-3.2} + \frac{3.36}{7-3.36} \approx 4.70.$$

3. Local Jacobians.

The flow operator is described in (31), hence the Jacobian with respect to ϕ is

$$G_\phi(\theta) = \frac{\partial \mathcal{G}}{\partial \phi} = \begin{bmatrix} 0 & 0 & 0 \\ p(\theta_1) & 0 & 0 \\ 1 - p(\theta_1) & q(\theta_2) & 0 \end{bmatrix}.$$

At θ_0 (i.e., $p_0 = q_0 = 0.8$):

$$G_\phi(\theta_0) = \begin{bmatrix} 0 & 0 & 0 \\ 0.8 & 0 & 0 \\ 0.2 & 0.8 & 0 \end{bmatrix}, \quad I - G_\phi(\theta_0) = \begin{bmatrix} 1 & 0 & 0 \\ -0.8 & 1 & 0 \\ -0.2 & -0.8 & 1 \end{bmatrix}.$$

The Jacobian w.r.t. θ is obtained from

$$\frac{\partial \mathcal{G}}{\partial \theta_1} = \begin{bmatrix} 0 \\ (\partial_{\theta_1} p) \phi_1 \\ -(\partial_{\theta_1} p) \phi_1 \end{bmatrix}, \quad \frac{\partial \mathcal{G}}{\partial \theta_2} = \begin{bmatrix} 0 \\ 0 \\ (\partial_{\theta_2} q) \phi_2 \end{bmatrix}.$$

Since $p(\theta_1) = \theta_1$ and $q(\theta_2) = \theta_2$, we have $\partial_{\theta_1} p = 1$, $\partial_{\theta_2} q = 1$. Using $\phi^{(0)} = (4, 3.2, 3.36)$, we obtain

$$G_\theta(\theta_0) = \begin{bmatrix} 0 & 0 \\ 4 & 0 \\ -4 & 3.2 \end{bmatrix}$$

4. Objective derivatives.

The objective $\mathcal{F}(\phi) = \sum_i \frac{\Lambda_i}{\mu_i - \Lambda_i}$ yields

$$\frac{\partial \mathcal{F}}{\partial \Lambda_i} = \frac{\mu_i}{(\mu_i - \Lambda_i)^2}.$$

Evaluated at $\phi^{(0)} = (4, 3.2, 3.36)$:

$$\frac{\partial \mathcal{F}}{\partial \Lambda_1} = \frac{6}{(6-4)^2} = 1.5, \quad \frac{\partial \mathcal{F}}{\partial \Lambda_2} = \frac{5}{(5-3.2)^2} \approx 1.5432, \quad \frac{\partial \mathcal{F}}{\partial \Lambda_3} = \frac{7}{(7-3.36)^2} \approx 0.5283.$$

Thus

$$\boxed{\partial_\phi \mathcal{F}(\phi^{(0)}) \approx [1.50 \ 1.54 \ 0.53]}, \quad \partial_\theta \mathcal{F}(\phi^{(0)}, \theta_0) = [0 \ 0],$$

since \mathcal{F} does not depend explicitly on θ .

5. Adjoint system.

The adjoint variable $y \in \mathbb{R}^3$ solves $(I - G_\phi(\theta_0))^\top y = (\partial_\phi \mathcal{F})^\top$.

We have

$$(I - G_\phi(\theta_0))^\top = \begin{bmatrix} 1 & -0.8 & -0.2 \\ 0 & 1 & -0.8 \\ 0 & 0 & 1 \end{bmatrix}, \quad (\partial_\phi \mathcal{F})^\top \approx \begin{bmatrix} 1.50 \\ 1.54 \\ 0.53 \end{bmatrix}.$$

Solving this upper-triangular system (back-substitution) yields

$$y_3 \approx 0.53, \quad y_2 \approx 1.54 + 0.8 y_3 \approx 1.97, \quad y_1 \approx 1.50 + 0.8 y_2 + 0.2 y_3 \approx 3.18.$$

Hence

$$\boxed{y \approx \begin{bmatrix} 3.18 \\ 1.97 \\ 0.53 \end{bmatrix}}.$$

6. Global gradient.

The implicit gradient is

$$\nabla_\theta J(\theta_0) = \partial_\theta \mathcal{F} + G_\theta(\theta_0)^\top y = G_\theta(\theta_0)^\top y.$$

Using

$$G_\theta(\theta_0)^\top y = \begin{bmatrix} 0 & 4 & -4 \\ 0 & 0 & 3.2 \end{bmatrix},$$

we obtain

$$\begin{aligned} \nabla_{\theta_1} J(\theta_0) &= 4y_2 - 4y_3 \approx 5.75, \\ \nabla_{\theta_2} J(\theta_0) &= 3.2 y_3 \approx 1.69. \end{aligned}$$

Thus

$$\boxed{\nabla_{\boldsymbol{\theta}} J(\boldsymbol{\theta}_0) \approx [5.75 \ 1.69]}.$$

7. Update and new cost.

With a step-size $\eta = 0.01$, the PG-Flow update is

$$\boldsymbol{\theta}_1 = \Pi_{\mathcal{U}} \left(\boldsymbol{\theta}_0 - \eta \nabla_{\boldsymbol{\theta}} J(\boldsymbol{\theta}_0) \right) = \Pi_{\mathcal{U}} \left(\begin{bmatrix} 0.8 \\ 0.8 \end{bmatrix} - 0.01 \begin{bmatrix} 5.7502 \\ 1.6906 \end{bmatrix} \right) \approx \begin{bmatrix} 0.7425 \\ 0.7831 \end{bmatrix}.$$

The corresponding routing probabilities are

$$p_1 = p(\boldsymbol{\theta}_{1,1}) \approx 0.7425, \quad q_1 = q(\boldsymbol{\theta}_{2,1}) \approx 0.7831.$$

The new steady-state flows are

$$\Lambda_1^{(1)} = 4, \quad \Lambda_2^{(1)} = 4p_1 \approx 2.97, \quad \Lambda_3^{(1)} = 4(1 - p_1 + q_1 p_1) \approx 3.36.$$

The updated cost is

$$J(\boldsymbol{\theta}_1) = \frac{4}{6-4} + \frac{\Lambda_2^{(1)}}{5 - \Lambda_2^{(1)}} + \frac{\Lambda_3^{(1)}}{7 - \Lambda_3^{(1)}} \approx 4.38.$$

Thus

$$J(\boldsymbol{\theta}_1) \approx 4.38 < J(\boldsymbol{\theta}_0) \approx 4.70,$$

which shows a strict decrease of the objective after a single PG-Flow iteration, in line with the monotone descent guarantee of Theorem 1.

B Appendix: EPN Network

Verification of the PG-Flow assumptions.

We verify assumptions (H1)–(H4) from Section 4.

(H1) The feasible control domain is a nonempty compact convex set. In the EPN model, the control vector $\alpha(\boldsymbol{\theta}) = (\alpha_1(\boldsymbol{\theta}), \dots, \alpha_N(\boldsymbol{\theta}))$ represents energy allocation intensities and B_{\max} is the maximum energy budget to be allocated across the network. Hence

$$\alpha_i(\boldsymbol{\theta}) \geq 0, \quad \sum_{i=1}^N \alpha_i(\boldsymbol{\theta}) \leq B_{\max},$$

defines a closed, bounded, and convex simplex under a budget constraint. In particular, the Euclidean projection onto this feasible set is well defined.

(H2) Since routing P is fixed and forms an open Jackson network, the DP flow system admits a unique solution.

(H3) In the EPN model, the steady-state DP flows ϕ_i^* satisfy the linear Jackson system $\phi^* = \lambda^{\text{ext}} + P^\top \phi^*$, whose solution does not depend on $\boldsymbol{\theta}$, since routing is fixed. Hence $\phi^*(\boldsymbol{\theta})$ is constant on \mathcal{U} and therefore coordinate-wise non-decreasing. Moreover, the EP flows are given by $\beta_i(\boldsymbol{\theta}) = \frac{\alpha_i(\boldsymbol{\theta})}{\gamma_i + \mu_i}$, and since $\alpha_i(\boldsymbol{\theta})$ is affine and non-decreasing in each component of $\boldsymbol{\theta}$, so is $\beta_i(\boldsymbol{\theta})$. Thus the steady-state flow vector

$$\phi^*(\boldsymbol{\theta}) = (\phi_1^*, \dots, \phi_N^*, \beta_1(\boldsymbol{\theta}), \dots, \beta_N(\boldsymbol{\theta}))$$

is coordinate-wise non-decreasing in $\boldsymbol{\theta}$, and (H3) holds.

(H4) For each node i , the local cost $r_i(\phi_i, \beta_i) = \frac{\phi_i}{\mu_i \beta_i - \phi_i}$ is convex and non-increasing in β_i for fixed ϕ_i , while the leakage term $\gamma_i \beta_i(\boldsymbol{\theta})$ is linear. In the present EPN model, the DP flows ϕ_i^* are independent of $\boldsymbol{\theta}$ and the EP flows $\beta_i(\boldsymbol{\theta})$ are affine in $\boldsymbol{\theta}$. Hence the composed map

$$\boldsymbol{\theta} \mapsto r_i(\phi_i^*, \beta_i(\boldsymbol{\theta}))$$

is convex in $\boldsymbol{\theta}$, even though $r_i(\phi_i, \beta_i)$ is not jointly convex in (ϕ_i, β_i) as stipulated in (H4). Summing over all nodes yields a convex objective $J(\boldsymbol{\theta})$, so the conclusion of (H4) holds for this EPN example.

Since (H1)–(H4) are satisfied, PG–Flow applies directly and produces globally convergent updates of the energy input parameters $\alpha_i(\boldsymbol{\theta})$ in this EPN.

Numerical Example: 5-node Energy Packet Network

We now consider a concrete EPN composed of $N = 5$ nodes. Data packets (DPs) circulate according to a fixed routing matrix P , while Energy packets arrivals are controlled through $\alpha_i(\boldsymbol{\theta}) = \theta_i$. The global constraint $\sum_{i=1}^N \alpha_i(\boldsymbol{\theta}) \leq B_{\max}$ recalls that a finite energy budget must be allocated across the network. This example illustrates PG–Flow on a topology containing multiple cycles.

DP dynamics. External arrivals occur at rates

$$\lambda^{\text{ext}} = (2.0, 1.0, 0.5, 0.5, 1.0).$$

Each DP served from node i is sent to node j with probability $P_{i,j}$, or leaves the network. The routing probabilities are:

- Node 1: $P_{1,2} = 0.6$, exit with prob. 0.4;
- Node 2: $P_{2,3} = 0.5$, $P_{2,4} = 0.3$, exit with prob. 0.2;
- Node 3: $P_{3,1} = 0.2$, $P_{3,5} = 0.5$, exit with prob. 0.3;
- Node 4: $P_{4,5} = 0.7$, exit with prob. 0.3;
- Node 5: $P_{5,3} = 0.4$, exit with prob. 0.6.

This corresponds to the routing matrix:

$$P = \begin{pmatrix} 0 & 0.6 & 0 & 0 & 0 \\ 0 & 0 & 0.5 & 0.3 & 0 \\ 0.2 & 0 & 0 & 0 & 0.5 \\ 0 & 0 & 0 & 0 & 0.7 \\ 0 & 0 & 0.4 & 0 & 0 \end{pmatrix}.$$

EP dynamics Maximum energy budget is fixed to 25 EPs. We take:

$$\mu = (10, 10, 5, 5, 5), \quad \gamma_i = 1 \quad \forall i.$$

Thus

$$\beta_i(\boldsymbol{\theta}) = \frac{\theta_i}{\gamma_i + \mu_i} = \frac{\theta_i}{\mu_i + 1}.$$

We initialise at

$$\boldsymbol{\theta}^{(0)} = (5, 5, 5, 5, 5), \quad \boldsymbol{\beta}^{(0)} \approx (0.4545, 0.4545, 0.8333, 0.8333, 0.8333).$$

Hence the effective DP service rate is

$$\mu_i \beta_i^{(0)} \approx (4.545, 4.545, 4.167, 4.167, 4.167).$$

In the following we give essential steps of the first iteration of PG-Flow.

1. DP flow equations

The DP flows satisfy the Jackson system $(I - P^\top)\boldsymbol{\phi} = \lambda^{\text{ext}}$. Contrary to an acyclic Jackson network, where the DP flows can be computed in linear algorithmic complexity, the presence of cycles in the routing matrix prevents such a reduction. Therefore, the steady-state flows are obtained with an iterative fixed-point method, whose per-iteration cost is $O(d^2)$ (and whose overall complexity depends on the number of iterations required). One may also use a direct dense linear solver (e.g., Gaussian elimination) with a cubic cost $O(d^3)$.

$$\boldsymbol{\phi}^* \approx (2.64, 2.58, 3.19, 1.27, 3.48).$$

And the stability holds since $\mu_i \beta_i^{(0)} > \phi_i^*$ for all i .

2. Performance at the initial point

The mean DP queue lengths are

$$D_i(\boldsymbol{\theta}) = \frac{\phi_i^*}{\mu_i \beta_i(\boldsymbol{\theta}) - \phi_i^*},$$

giving

$$D(\boldsymbol{\theta}^{(0)}) = \sum_i D_i(\theta^{(0)}) \approx 11.49.$$

The EP leakage cost is

$$L(\boldsymbol{\theta}^{(0)}) = \sum_i \gamma_i \beta_i^{(0)} \approx 3.41.$$

With $w_1 = w_2 = 1$,

$$J(\boldsymbol{\theta}^{(0)}) = D(\boldsymbol{\theta}^{(0)}) + L(\boldsymbol{\theta}^{(0)}) \approx 14.90.$$

3. Gradient and adjoint

We compute

$$\frac{\partial \mathcal{F}}{\partial \phi_i} = \frac{\mu_i \beta_i}{(\mu_i \beta_i - \phi_i)^2}, \quad \frac{\partial \mathcal{F}}{\partial \beta_i} = -\frac{\mu_i \phi_i}{(\mu_i \beta_i - \phi_i)^2} + \gamma_i.$$

At $(\boldsymbol{\phi}^*, \boldsymbol{\beta}^{(0)})$:

$$\begin{aligned} \frac{\partial \mathcal{F}}{\partial \boldsymbol{\phi}} &\approx (1.25, 1.18, 4.37, 0.50, 8.84), \\ \frac{\partial \mathcal{F}}{\partial \boldsymbol{\beta}} &\approx (-6.27, -5.68, -15.72, 0.24, -35.90). \end{aligned}$$

The PG-Flow adjoint solves

$$(I - P)y^\phi = \left(\frac{\partial F}{\partial \phi} \right)^\top.$$

This gives

$$y^\phi \approx (7.68, 10.72, 12.90, 10.30, 13.99), \quad y^\beta = \left(\frac{\partial F}{\partial \beta} \right)^\top.$$

The gradient is

$$\frac{\partial J}{\partial \theta_i} = \frac{y_i^\beta}{\mu_i + 1},$$

yielding

$$\nabla_{\boldsymbol{\theta}} J(\boldsymbol{\theta}^{(0)}) \approx (-0.57, -0.52, -2.62, 0.04, -5.98).$$

4. Update and new cost

With step-size $\eta = 0.05$:

$$\boldsymbol{\theta}^{(1)} = \Pi_{\mathcal{U}} \left(\boldsymbol{\theta}^{(0)} - \eta \nabla J(\boldsymbol{\theta}^{(0)}) \right) \approx (4.931, 4.928, 5.032, 4.900, 5.206).$$

Re-evaluating the cost:

$$D(\boldsymbol{\theta}^{(1)}) \approx 10.47, \quad L(\boldsymbol{\theta}^{(1)}) \approx 3.42,$$

$$J(\boldsymbol{\theta}^{(1)}) \approx 13.89 < J(\boldsymbol{\theta}^{(0)}) \approx 14.90.$$